environmental microbiology

Environmental Microbiology (2020) **22**(12), 5280–5299 doi:10.1111/1462-2920.15216

# Common plant flavonoids prevent the assembly of amyloid curli fibres and can interfere with bacterial biofilm formation

**Mihaela Pruteanu,[1] José I. Hernández Lobato,[1] Thomas Stach[2] and Regine Hengge[1]***

[1]*Institut für Biologie/Mikrobiologie, Humboldt-Universität zu Berlin, Berlin, 10115, Germany.*

[2]*Institut für Biologie/Zoologie, Humboldt-Universität zu Berlin, Berlin, 10115, Germany.*

## Summary

**Like all macroorganisms, plants have to control bacterial biofilm formation on their surfaces. On the other hand, biofilms are highly tolerant against antimicrobial agents and other stresses. Consequently, biofilms are also involved in human chronic infectious diseases, which generates a strong demand for anti-biofilm agents. Therefore, we systematically explored major plant flavonoids as putative anti-biofilm agents using different types of biofilms produced by Gram-negative and Gram-positive bacteria. In *Escherichia coli* macrocolony biofilms, the flavone luteolin and the flavonols myricetin, morin and quercetin were found to strongly reduce the extracellular matrix. These agents directly inhibit the assembly of amyloid curli fibres by driving CsgA subunits into an off-pathway leading to SDS-insoluble oligomers. In addition, they can interfere with cellulose production by still unknown mechanisms. Submerged biofilm formation, however, is hardly affected. Moreover, the same flavonoids tend to stimulate macrocolony and submerged biofilm formation by *Pseudomonas aeruginosa*. For *Bacillus subtilis*, the flavonone naringenin and the chalcone phloretin were found to inhibit growth. Thus, plant flavonoids are not general anti-biofilm compounds but show species-specific effects. However, based on their strong and direct anti-amyloidogenic activities, distinct plant flavonoids may provide an attractive strategy to specifically combat amyloid-based biofilms of some relevant pathogens.**

Received 22 June, 2020; revised 25 August, 2020; accepted 27 August, 2020. *For correspondence. E-mail regine.hengge@hu-berlin.de; Tel. (49)-30-2093-49686; Fax (49)-30-2093-49682.

## Introduction

Bacterial biofilms are ubiquitous communities of bacterial cells embedded in a self-produced matrix of extracellular polymeric substances (EPS) (Flemming and Wuertz, 2019). By forming biofilms, bacteria can colonize diverse abiotic and biotic surfaces. Therefore, macroorganisms have to protect their surfaces or at least control this colonization, for instance by interfering with bacterial EPS formation. Matrix EPS include various exopolysaccharides, secreted proteins some of which can form amyloid fibres, extracellular DNA and lipids (Flemming and Wingender, 2010). A widely occurring bacterial exopolysaccharide is cellulose, which by many bacteria is produced as a phosphoethanolamine (pEtN)-modified derivative (Thongsomboon *et al*., 2018; Serra and Hengge, 2019a). By forming a cohesive polymer network, matrix components mediate bacterial surface adhesion, provide for mechanical stability of biofilms and protect bacteria against the detrimental effects of chemical insults and other environmental challenges (Flemming and Wingender, 2010). Bacterial cells within biofilms are physiologically highly heterogeneous, with spatially organized subpopulations co-existing in various stages of growth, including multiple stress-resistant cells in the large stationary phase zones of biofilms (Stewart and Franklin, 2008; Serra and Hengge, 2014; Hengge, 2020). With these subpopulations also differing in matrix production, complex matrix architectures are built that are crucial for the tissue-like cohesion and elasticity of biofilms, which leads to the typical macroscopic wrinkling of growing macrocolony biofilms (Serra *et al*., 2015; Klauck *et al*., 2018; Serra and Hengge, 2019b).

By trapping certain antibiotics or other toxic molecules and shielding and 'glueing' together bacterial cells, the extracellular matrix is also a key factor in the tolerance of bacterial biofilms against antimicrobial therapy and host immune systems (Anderson and O'Toole, 2008; Hall and Mah, 2017). Because of this pronounced tolerance, biofilms of pathogenic bacteria play crucial roles in most chronic infections as well as in the colonization of indwelling medical devices and orthopaedic implants (Costerton *et al*., 1999; Römling *et al*., 2014). As a consequence, there is an urgent

need for anti-biofilm agents that are intensively searched for by screening large chemical libraries (Peach *et al*., 2011) or natural products originating from plants, marine sponges, or other biological sources (Stowe *et al*., 2011; Khan and Lee, 2015; Lu *et al*., 2019). Anti-biofilm compounds are active at concentrations that do not interfere with bacterial growth or survival but prevent biofilm formation or disperse preformed biofilms. They can target the matrix EPS or regulatory processes (Rabin *et al*., 2015; Koo *et al*., 2017; Roy *et al*., 2018).

Plants are an excellent source of anti-biofilm compounds, as they have to control bacterial growth on their surfaces (Nunes Silva *et al*., 2016). However, instead of making '*tabula rasa*' that could open new niches for phytopathogenic bacteria, they produce secondary metabolites to control bacterial surface colonization and biofilm formation, thereby managing their microbiota (Tyler and Triplett, 2008; Vorholt, 2012; Bulgarelli *et al*., 2013; Hengge, 2019). Enteric bacteria, which include many pathogenic variants of, e.g., *E. coli*, *Salmonella* or *Klebsiella*, spend part of their life cycle in the environment and are well equipped to form biofilms on plants, which by plant consumption opens a route back into humans or animals.

Two major EPS components of enteric bacteria, i.e. amyloid curli fibres as well as pEtN-cellulose, are involved in bacterial attachment to plant surfaces (Jeter and Matthysse, 2005; Macarisin *et al*., 2012; Yaron and Römling, 2014). In contrast to the toxic amyloids associated, e.g., with human neurodegenerative diseases, curli fibres are functional amyloids (Romero and Kolter, 2014). Amyloids share a cross-beta core structure irrespective of the amino acid sequence of the native protein, making them an attractive and potentially broad-spectrum target for anti-biofilm compounds (Cegelski *et al*., 2009; Andersson *et al*., 2013; Romero *et al*., 2013; Perov *et al*., 2019). Also beyond enterics, amyloid or amyloid-like protein fibres are found in the biofilm matrices of Gram-negative and Gram-positive bacteria (Larsen *et al*., 2007; Taglialegna *et al*., 2016). These include Fab fibres in many *Pseudomonas* species (Zeng *et al*., 2015; Rouse *et al*., 2018), TasA fibres in *B. subtilis* (Diehl *et al*., 2018; Erskine *et al*., 2018), naturally occurring fragments of the cell-surface-localized adhesins P1 and WapA and the secreted SMU_63c protein in *Streptococcus mutans* (Besingi *et al*., 2017; Berdon-Barran *et al*., 2020) and phenol-soluble modulins in *Staphylococcus aureus* (Marinelli *et al*., 2016; Salinas *et al*., 2018).

In *E. coli* and related bacteria, curli subunits and the assembly machinery are encoded in the divergent operons *csgBAC* and *csgDEFG*, with *csgA* coding for the major structural subunit protein. CsgA is secreted to the cell surface as unstructured and soluble monomers (Gibson *et al*., 2007) that are then templated into ordered amyloid fibres by the nucleator protein CsgB (Hammer *et al*., 2007; Evans and Chapman, 2014). Curli fibres are produced either alone or in combination with pEtN-cellulose by most commensal and pathogenic *E. coli* strains (Bokranz *et al*., 2005; Serra *et al*., 2013a; Thongsomboon *et al*., 2018; Serra and Hengge, 2019a). As a biofilm master regulator, CsgD activates the expression of genes essential for curli and pEtN-cellulose production during entry into the stationary phase, since CsgD expression depends on the stationary phase sigma subunit of RNA polymerase, RpoS ($\sigma^S$), and the second messenger c-di-GMP (Hengge, 2009, 2011). Therefore, also these regulators and c-di-GMP could be potential anti-biofilm targets.

Flavonoids are plant secondary metabolites with numerous functions in plant physiology and development, including oxidative stress protection and signalling, pigmentation, UV protection, defence and plant-microbe signalling (Falcone Ferreyra *et al*., 2012; Mouradov and Spangenberg, 2014; Mathesius, 2018). They are known for their antioxidant, anti-inflammatory, antibacterial, antiviral, antiprotozoan, antifungal, anticancer and anti-allergic properties that can promote human health and reduce the risk of diseases (Havsteen, 2002; Cushnie and Lamb, 2005, 2011; Gorniak and Bartoszewski, 2019). Although their anti-biofilm properties have been explored in recent years (Lee *et al*., 2011; Manner *et al*., 2013; Coppo and Marchese, 2014; Nunes Silva *et al*., 2016; Barbieri *et al*., 2017; Francolini and Piozzi, 2019; Khameneh *et al*., 2019; Memariani *et al*., 2019), their mechanism of action at the molecular level has not been investigated systematically. In our study, we therefore aimed at a systematic exploration of anti-biofilm activities of common plant flavonoids on different types of biofilms produced by Gram-negative and Gram-positive bacteria. We show here that flavonoids are not general anti-biofilm compounds, but rather specific anti-amyloidogenic agents that can reduce enteric biofilms by directly interfering with the assembly of CsgA subunits into amyloid fibres.

## Results

### *Distinct flavonoids inhibit macrocolony biofilm formation of* E. coli

Flavonoids contain a $C_6$-$C_3$-$C_6$ carbon framework (phenyl benzopyran), which—depending on the oxidation state, the degree of saturation and the substituents present on the benzopyran core—defines subclasses such as flavones, isoflavones, flavonols, flavanones, flavanols, chalcones and anthocyanins (Rauter *et al*., 2018). We selected 15 common plant flavonoids, which represent different

subclasses (Fig. 1), to explore their anti-biofilm properties against *E. coli* macrocolony biofilms.

The specific morphological patterns of *E. coli* K12 macrocolony biofilms are indicative of the presence of curli fibres and pEtN-cellulose in the biofilm matrix (Serra *et al*., 2013a; Serra and Hengge, 2014). Therefore, these morphological patterns together with Congo red (CR) staining of both matrix components are an excellent phenotypic readout for biofilm formation, allowing to visually analyse the production and regulation of curli fibres and pEtN-cellulose (Serra and Hengge, 2017). For our study, we used three *E. coli* K-12 strains with well-characterized macrocolony morphology: (i) strain W3110 produces only amyloid curli fibres which generates macrocolony biofilms with a concentric ring pattern and dark red staining with CR (Serra *et al*., 2013b); (ii) strain AR3110, a W3110 derivative with restored ability to synthesize pEtN-cellulose (Serra *et al*., 2013a; Thongsomboon *et al*., 2018), forms large and flat curli- and pEtN-cellulose-containing macrocolonies with long radial ridges and small wrinkles that also stain dark red with CR; and (iii) strain AR282, a *ΔcsgBA* derivative of AR3110, produces pEtN-cellulose only, which results in macrocolonies with small interwined wrinkles that stain pink with CR. As a growth control, i.e. in order to probe the antimicrobial potential of the flavonoids, we used strain AP303, a W3110 *ΔcsgBA::kan* derivative, or GBK5, a *ΔcsgD* derivative of W3110, which both do not produce curli fibres nor pEtN-cellulose. Since CsgD is hardly present above 30°C in *E. coli* K-12, macrocolony biofilms on agar plates were grown at 28°C.

The flavone luteolin (3′,4′,5,7-tetrahydroxyflavone) exerted a strong and dose-dependent inhibition of macrocolony morphogenesis and CR staining, whereas no reduction of colony growth was observed with the control strain AP303 (Fig. 2). This indicated a clear reduction in both curli and pEtN-cellulose production. The free hydroxyl groups on positions 3′ and 4′ are important for this anti-biofilm activity since the luteolin 3′- or 4′-methyl ether derivatives (chrysoeriol and diosmetin respectively), as well as apigenin (4′,5,7-trihydroxyflavone) with only 4′-OH, did not show the inhibitory effect on matrix-dependent macrocolony morphogenesis (Fig. 3). Moreover, chrysin (5,7-dihydroxyflavone) with no hydroxyl groups at these positions, displayed no anti-biofilm activity at all (Fig. S1). Also the isoflavones, daidzein and

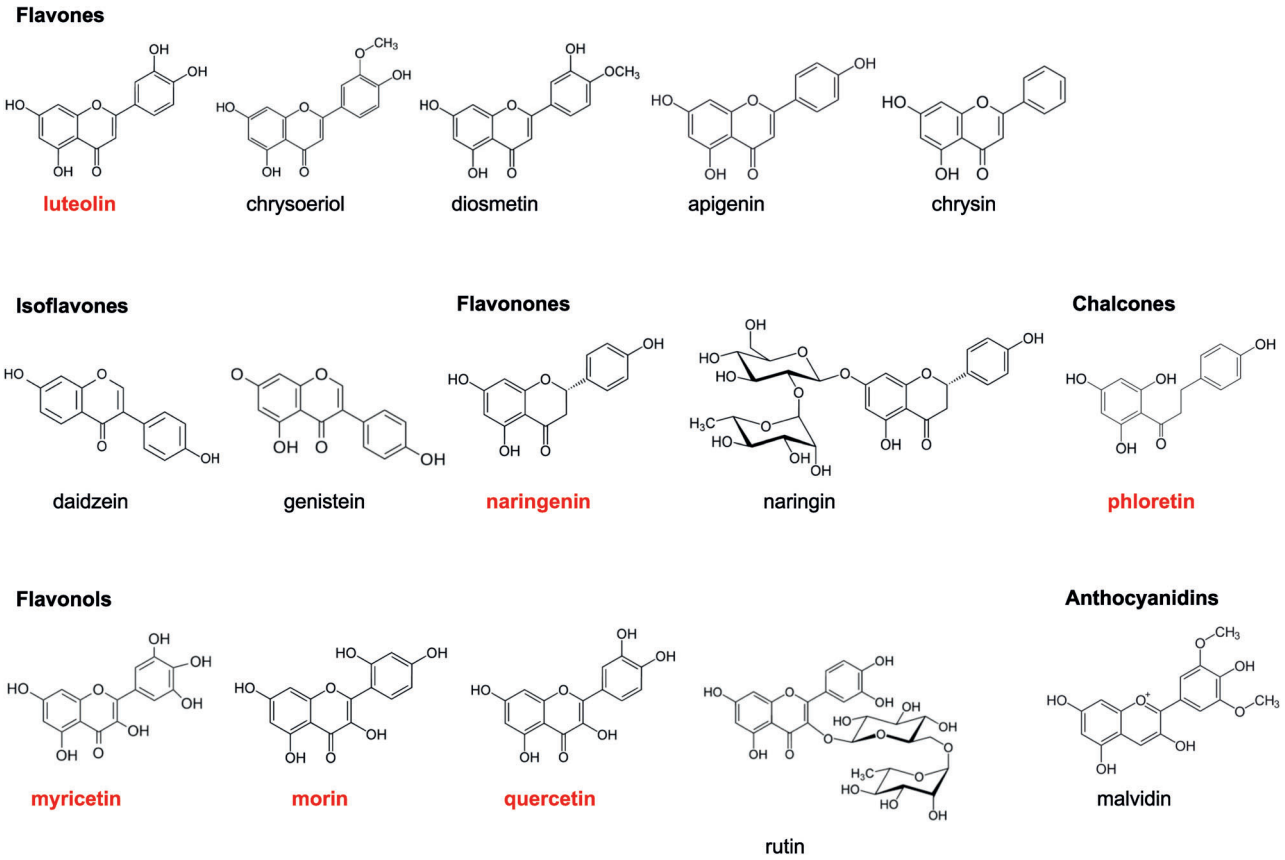


**Fig. 1.** Chemical structures of the flavonoids used in this study. Flavonoids found to exhibit anti-biofilm activity in macrocolony biofilm assays are marked in red.

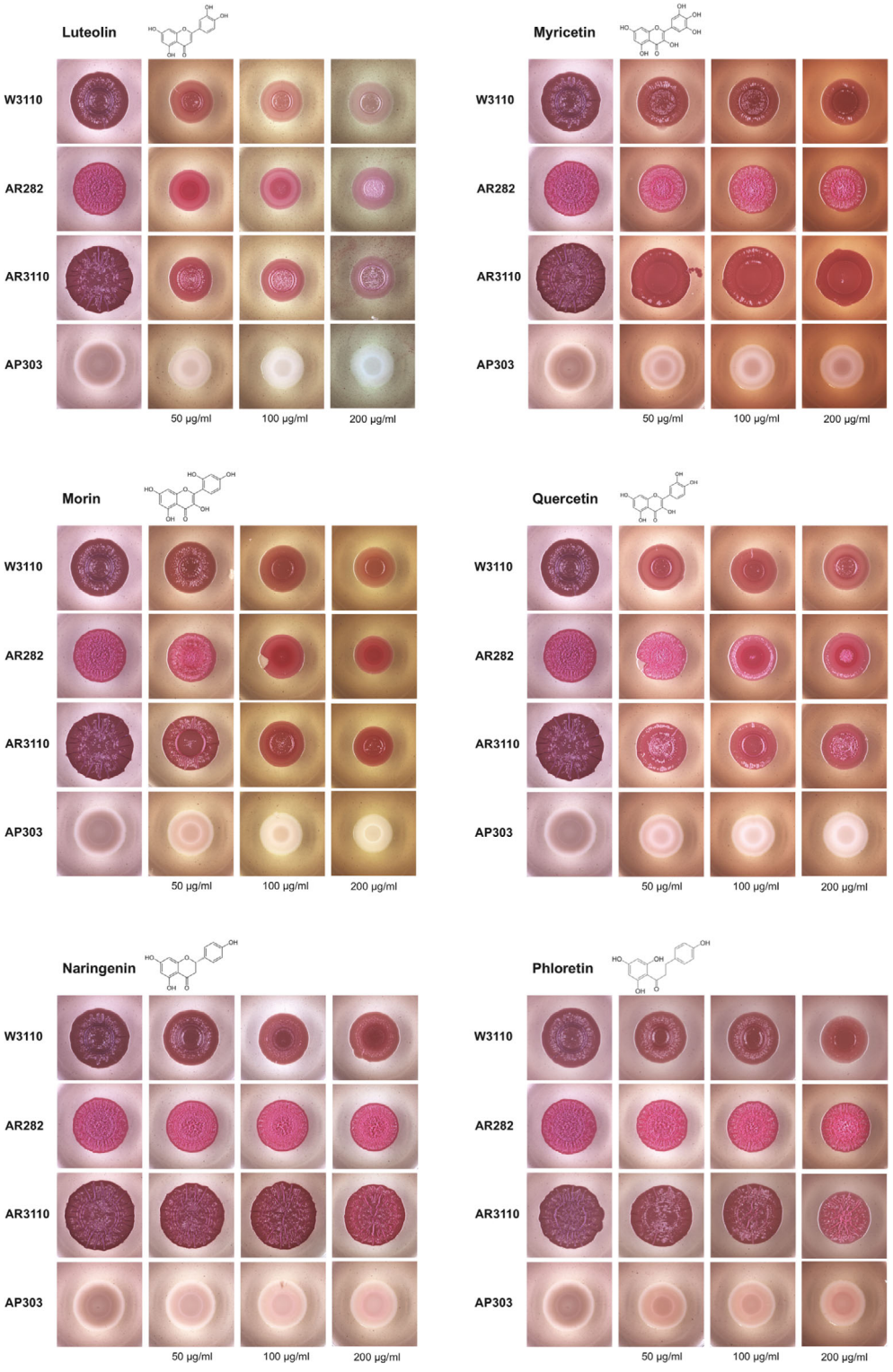


**Fig. 2.** Flavonoids reduce the formation of curli fibres and pEtN-cellulose in *E. coli* K-12 macrocolony biofilms. Images show macrocolony biofilms of strains W3110 (which produces curli only), AR282 (pEtN-cellulose only), AR3110 (curli and pEtN-cellulose) and the growth control strain AP303 (neither curli nor pEtN-cellulose) grown for 5 days at 28°C on CR plates in the presence or absence of the different flavonoids at the indicated concentrations.

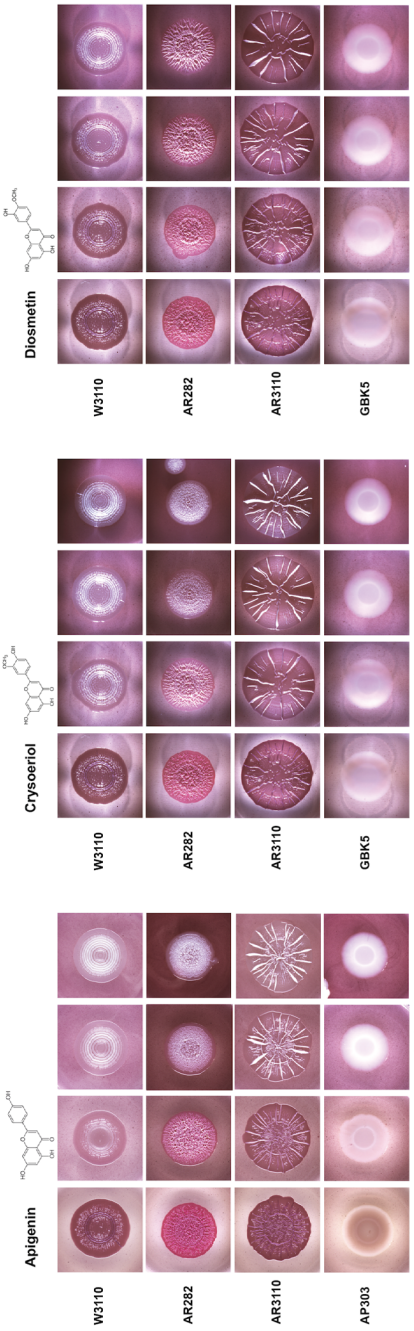


**Fig. 3.** Apigenin and 3′- or 4′-methyl ether derivatives of luteolin (chrysoeriol and diosmetin respectively) reduce Congo red binding but stimulate matrix-dependent morphogenesis of *E. coli* K-12 macrocolony biofilms. Images show macrocolony biofilms of strains W3110, AR282, AR3110 and the growth control strains AP303 or GBK3 (both not producing curli nor pEtN-cellulose) grown for 5 days at 28°C on CR-plates in the presence or absence of apigenin, chrysoeriol and diosmetin at the indicated concentrations.

genistein, with only a 4′-OH group, but no 3′-OH group, did not affect macrocolony morphology, confirming the importance of these hydroxyl groups for anti-biofilm activity (Fig. S1). Notably, apigenin, chrysoeriol and diosmetin even seemed to promote macrocolony morphogenesis somewhat—particularly visible with AR3110, which generated fewer, but higher ridges, which is typical for increased matrix production (Serra and Hengge, 2019b)—while at the same time reducing CR binding, i.e. the macroscopic structures of the macrocolonies tended to remain white on CR plates (Fig. 3). This suggests that these compounds compete with CR binding to the EPS components but—in contrast to luteolin (Fig. 2)—do not interfere with their assembly.

The flavonols myricetin, morin and quercetin reduced curli production in a dose-dependent manner, and also a decrease in pEtN-cellulose was observed with morin and quercetin at higher concentrations (100 and 200 μg ml$^{-1}$; Fig. 2). Rutin, a glycosylated form of quercetin (quercetin 3-rhamnosidoglucoside), did not show any anti-biofilm activity (Fig. S1). Curli production was also reduced by the flavonone naringenin at higher concentrations (100 and 200 μg ml$^{-1}$), whereas pEtN-cellulose was not affected (Fig. 2). Unlike myricetin, which reduced curli production in both W3110 and AR3110 strains (with no effect on pEtN-cellulose), naringenin (at 200 μg ml$^{-1}$) only slightly affected the macrocolony structure in AR3110 strain, where pEtN-cellulose was produced. Also for naringenin, the glycosylated derivative naringin (naringenin 7-rhamnosidoglucoside), was not effective against biofilm formation (Fig. S1). For the chalcone phloretin a relatively weak anti-biofilm activity, affecting the formation of curli fibres only, was observed at high concentration (200 μg ml$^{-1}$; Fig. 2). The anthocyanidin malvidin had no anti-biofilm activity in our macrocolony system (Fig. S1).

These data show that distinct flavonoids reduce biofilm matrix components, with some compounds reducing or even eliminating both curli fibres and pEtN-cellulose while others affect curli fibres only. Whether this is the result of the altered synthesis of these matrix components and/or their assembly is analysed further below.

### *Flavonoids with anti-biofilm activity do not reduce/inhibit the expression of matrix genes but prevent curli subunit polymerization directly*

To determine whether altered gene expression is the underlying mechanism of reduced curli and pEtN-cellulose production in the presence of specific flavonoids (Fig. 2), we tested the expression of the relevant genes using single-copy *lacZ* reporter fusions to *csgB* (the first gene in the curli biosynthesis *csgBAC* operon) and *dgcC*. DgcC is a diguanylate cyclase required to specifically activate cellulose synthase BcsA, which is

allosterically controlled by c-di-GMP binding to its PilZ domain (García *et al*., 2004; Morgan *et al*., 2014; Richter *et al*., 2020). Transcription of both the *csgBAC* operon and *dgcC* requires the biofilm regulator CsgD (Römling *et al*., 2000; Brombacher *et al*., 2003), whose expression in turn depends on the stationary phase sigma factor RpoS and additional complex c-di-GMP input (Lindenberg *et al*., 2013; Sarenko *et al*., 2017; Pfiffer *et al*., 2019). As a consequence, matrix production by *E. coli* occurs during the transition into the stationary phase, both in starved macrocolony biofilm zones as well as in liquid cultures running out of nutrients (Pesavento *et al*., 2008; Serra and Hengge, 2014; Klauck *et al*., 2018).

None of the flavonoids with anti-biofilm activity reduced or inhibited *csgB* or *dgcC* expression in stationary phase cultures of *E. coli* (Fig. S2). Therefore, we reasoned that reduced curli production in macrocolony biofilms in the presence of these flavonoids could be the result of direct interference with the assembly of curli fibres, i.e. CsgA polymerization. To investigate this, we monitored the kinetics of CsgA polymerization *in vitro* using the strongly increased fluorescence of thioflavin-T (ThT) observed upon its binding to the β-sheet-rich structures of amyloid CsgA fibres assembling *in vitro* (Wang *et al*., 2007; Zhou *et al*., 2013).

CsgA was purified in a soluble, unstructured state (Fig. S3) and allowed to polymerize for 16 h in the presence or absence of the flavonoids that had shown a clear effect on curli fibres *in vivo* (Fig. 2). CsgA polymerization displayed a typical sigmoidal response with the increase in ThT fluorescence—reflecting curli fibre assembly—after a lag time of about 2 h and a final plateau after 6–8 h (in the solvent control containing DMSO alone; Fig. 4). Note that the typical lag phase in this *in vitro* assay is due to the initial absence of an amyloid template, which *in vivo* would be provided by CsgB. Adding increasing concentrations of luteolin to freshly purified monomeric CsgA increased this lag phase and inhibited the assembly of CsgA subunits into curli fibres in a dose-dependent manner, with the highest concentration used in the macrocolony assays (200 μg ml$^{-1}$, corresponding to 698 μM) abolishing curli fibre formation completely (Fig. 4; panels on the left side show the effects of flavonoids at the highest concentrations used in macrocolony biofilms). Myricetin prevented curli fibres assembly even at 200 μM already, thus being a strong inhibitor of CsgA polymerization (Fig. 4). In the case of morin, its autofluorescence resulted in the higher basal fluorescence level at 200 and 662 μM compared with those at 50 and 100 μM. However, at 662 μM (200 μg ml$^{-1}$), also morin completely blocked CsgA polymerization (Fig. 4). Quercetin equally increased the lag phase to 4 h and strongly inhibited CsgA subunits assembly into curli fibres (Fig. 4). The very weak effect only of naringenin on *in vitro* curli fibre formation (Fig. 4) corresponded to a weak *in vivo* effect (Fig. 2).

Overall, the flavonoids with the strongest anti-biofilm activity in macrocolony biofilms (luteolin, myricetin, morin and quercetin; Fig. 2) prevented CsgA polymerization *in vitro* in a concentration-dependent manner (Fig. 4). However, these flavonoids did not maintain CsgA in a soluble monomeric state (Fig. S3), suggesting that in their presence CsgA forms SDS-insoluble off-pathway oligomers that cannot assembly into curli fibres. To confirm that these specific flavonoids inhibit CsgA polymerization and not ThT binding to the curli fibres, we performed transmission electron microscopy (TEM). CsgA was incubated for 16 h in the presence or absence of luteolin or myricetin, which were found to abolish curli formation in the ThT amyloid polymerization *in vitro* assays as shown above. CsgA assembled into TEM-detectable curli fibres in the absence of these compounds, and similar fibres were formed in the presence of ThT (Fig. 5). By contrast, curli fibres were undetectable by TEM when CsgA was incubated with the inhibitory compounds, regardless of the presence or absence of ThT (Fig. 5). Together, these data demonstrate that distinct plant flavonoids, in particular those with the strongest anti-biofilm activity in macrocolony biofilms, have direct anti-amyloidogenic properties, i.e. they prevent the assembly of CsgA subunits into curli fibres.

Interestingly, the moderately curli-reducing activity of the chalcone phloretin (Fig. 2) was found to be based on a different mechanism. *In vitro*, phloretin even accelerated the initial polymerization of CsgA, as evidenced by a shorter lag phase (compared to the DMSO control) when CsgA was incubated with 729 μM phloretin (200 μg ml$^{-1}$; Fig. 4). Since it also did not significantly reduce the expression of the curli operon (Fig. S2), we hypothesized that phloretin could reduce curli fibres in macrocolonies by possibly targeting CsgB, which *in vivo* first forms an SDS-insoluble amyloid, which remains cell surface-associated and then acts as a template for CsgA polymerization (Deshmukh *et al*., 2018). We therefore investigated whether phloretin affected the solubility of CsgB by immunoblotting samples derived from macrocolonies and/or the underlying agar support (Fig. 6). In phloretin-free macrocolony samples, the initially SDS-insoluble CsgB could be detected by SDS-PAGE and immunoblotting upon sample treatment with hexafluoroisopropanol (HFIP), but no CsgB was found after growth in the presence of phloretin (Fig. 6A). When samples contained both cells from the macrocolony as well as a plug from the underlying agar, CsgB was detected after growth in the presence of phloretin and even did not require HFIP-mediated solubilization (Fig. 6B). If agar plugs alone were analysed, this HFIP-independent soluble CsgB was again detected, especially after 3 days of growth (Fig. 6C). Taken together, these data show that in the presence of phloretin, CsgB is released from the cells and

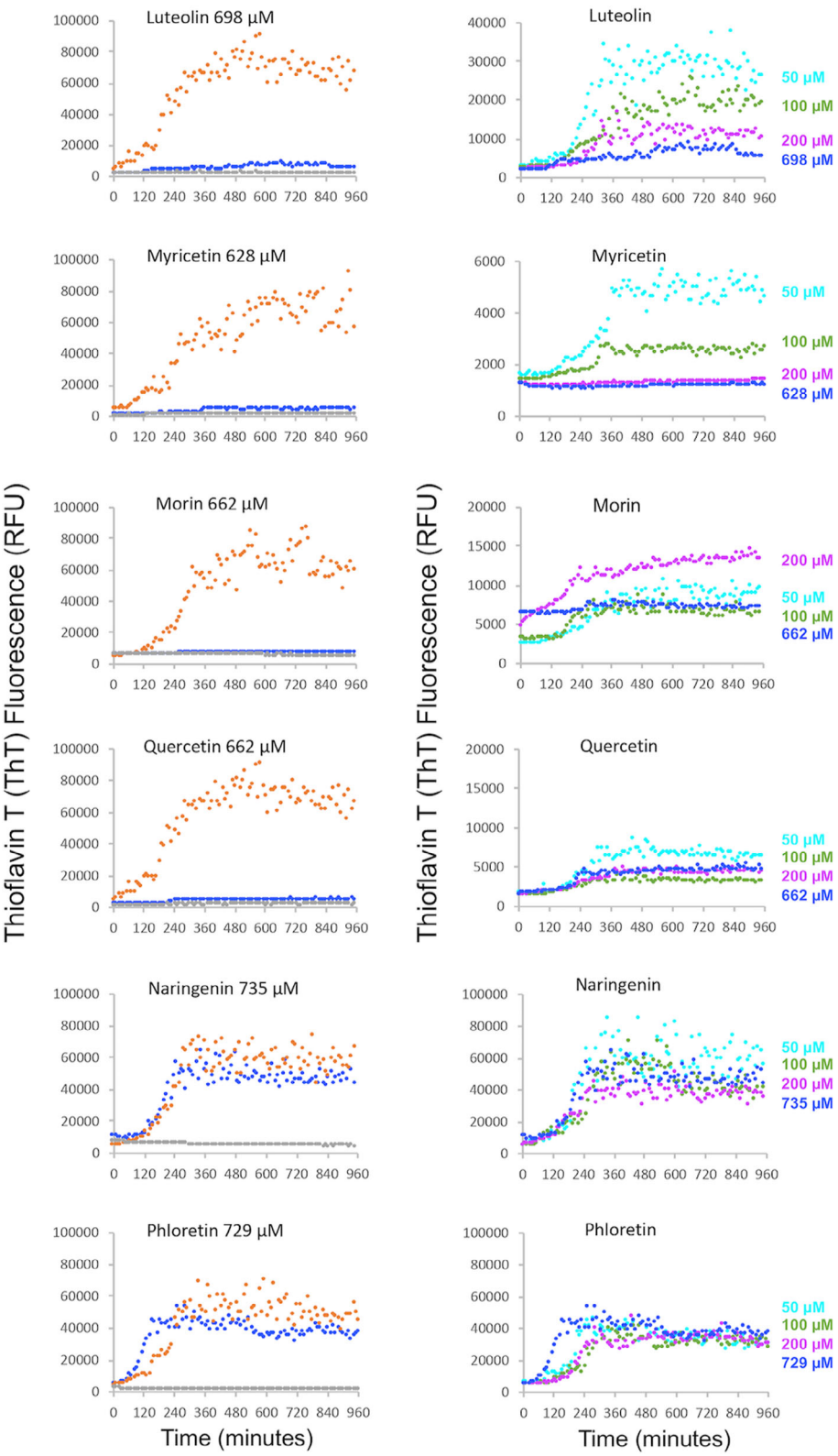


**Fig. 4.** Flavonoids inhibit *in vitro* CsgA polymerization measured by ThT fluorescence. The fluorescence of 20 µM ThT mixed with freshly purified CsgA, in the presence or absence of the respective flavonoids, was measured at 495 nm after excitation at 438 nm. Data points recorded in 10-min intervals over a 16 h incubation period are displayed. Left panels: CsgA polymerization in the absence of flavonoids (DMSO controls; orange circles) and in the presence of 200 µg ml$^{-1}$ flavonoids (corresponding to different the µM concentrations given in the figure; blue circles); fluorescence in the KPi buffer containing 200 µg ml$^{-1}$ flavonoids (CsgA-free control; grey circles). 200 µg ml$^{-1}$ corresponds to the highest concentration used in the macrocolony biofilms (Fig. 1). Right panels: CsgA polymerization in the presence of increasing concentrations of flavonoids up to 200 µg ml$^{-1}$. The graphs shown are representative data sets of at least three replicates performed for each experiment.

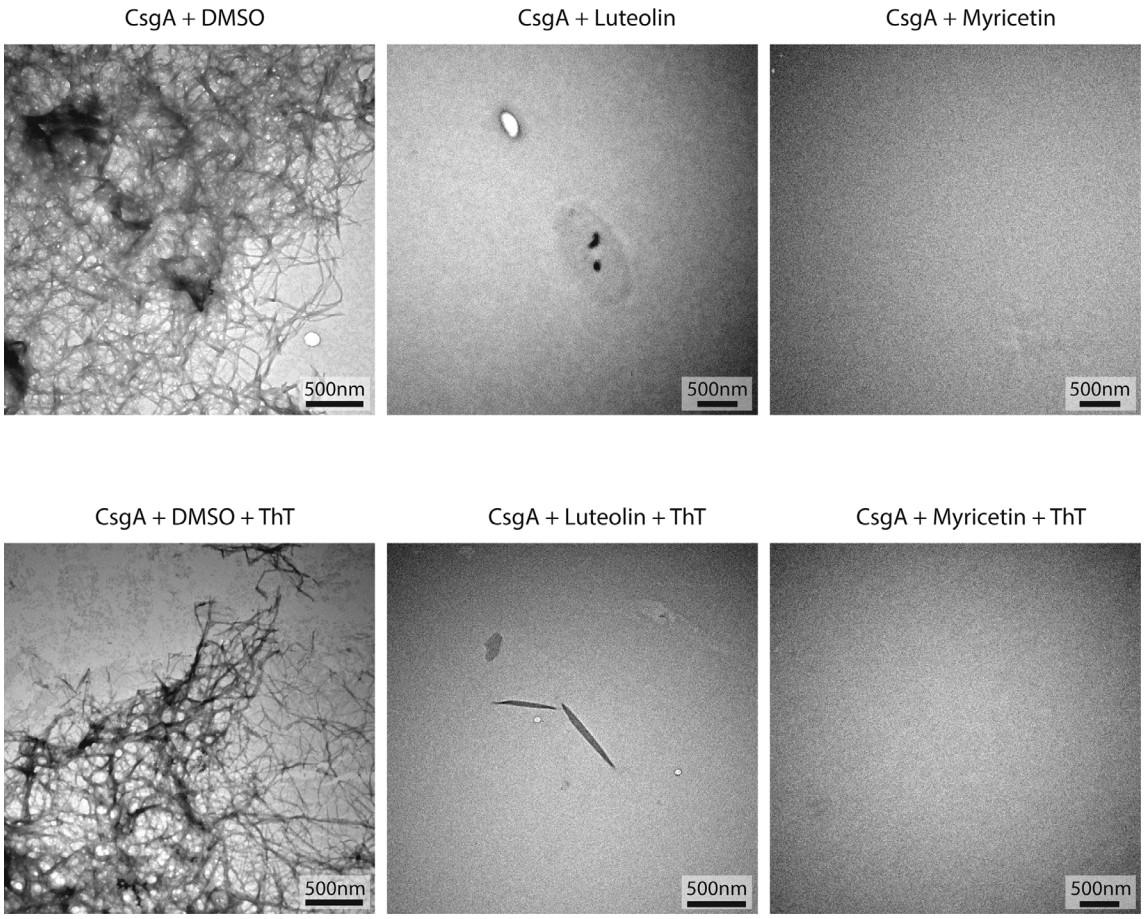


**Fig. 5.** Visual detection of curli fibres produced in polymerization assays with purified CsgA performed in the absence and presence of flavonoids. Transmission electron microscopy (TEM) of freshly purified CsgA incubated for 16 h revealed abundant fibres, whereas no curli fibres were detected when freshly purified CsgA was incubated for 16 h with the inhibitory flavonoids luteolin and myricetin. Images were taken after 16 h of incubation with or without ThT, in the presence and absence of the inhibitory compounds. Scale bars are shown in the lower right corners of the images.

remains in an SDS-soluble form, i.e. it does not fold into the amyloid conformation. As a consequence, the *in vivo* polymerization of CsgA into amyloid fibres is compromised since—unlike the slow spontaneous polymerization *in vitro*—this process depends on templating by the surface-attached amyloid form of CsgB.

### *Effects of flavonoids on macrocolony biofilms of pathogenic* E. coli *and other Gram-negative and Gram-positive bacteria*

In order to assess whether these flavonoids have anti-biofilm activity against other bacteria we tested their effects on macrocolony biofilm formation of an emerging enteric pathogen, the enteroaggregative *E. coli* (EAEC) strain 55989, the human opportunistic pathogen *Pseudomonas aeruginosa* (strain UCBPP-PA14), and the Gram-positive model organism *B. subtilis* (strain NCIB 3610). The macrocolony biofilms were grown at 28°C and 37°C in the absence or presence of 200 μg $ml^{-1}$ of the flavonoids (Fig. 7).

In comparison to the *E. coli* K-12 laboratory strain AR3110, the EAEC strain 55989 produces higher levels of CsgD as well as curli fibres and pEtN-cellulose also at 37°C (Richter *et al*., 2014). In general, the flavonoids had an inhibitory effect on EAEC-55989 macrocolony biofilms as observed for the K-12 strain AR3110 (at both 28°C and 37°C; note that the very weak residual matrix production of AR3110 at 37°C is also reduced by flavonoids), although at 28°C EAEC-55989 seemed somewhat less sensitive against the flavonoids (Fig. 7). Surprisingly, *P. aeruginosa* strain PA14 showed an increase in macrocolony wrinkling at 28°C in the presence of luteolin, myricetin and quercetin, suggesting enhanced production of extracellular matrix. This phenotype is reminiscent of that of a *P. aeruginosa* PA14 mutant lacking certain phenazines (Dietrich *et al*., 2013; Kempes *et al*., 2014). Interestingly, luteolin also seemed to induce phenazine production as evidenced by macrocolonies turning green (Fig. 7). These effects on *P. aeruginosa* macrocolony morphology and colour were not observed at 37°C. Biofilm

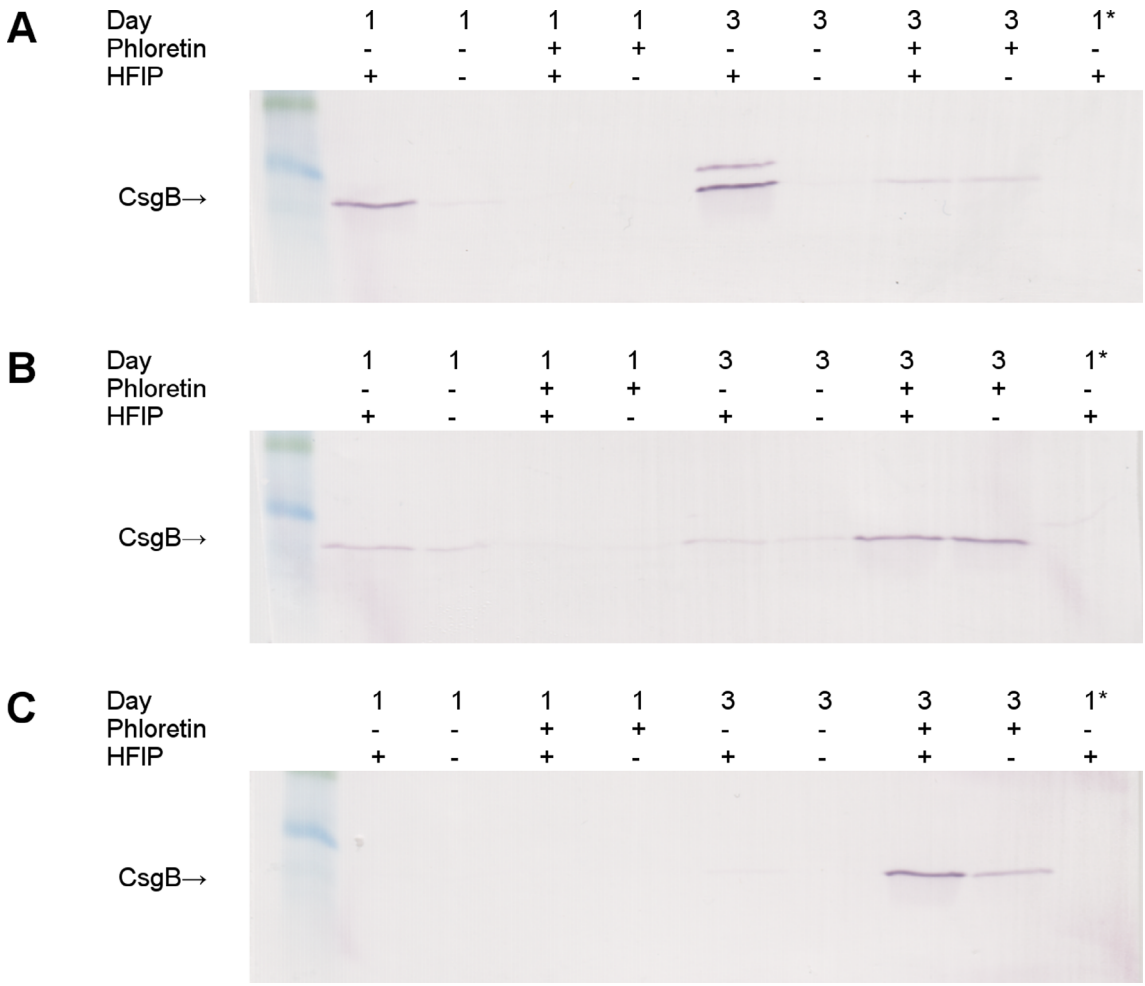


**Fig. 6.** Growth of macrocolony biofilms in the presence of phloretin results in a release of non-amyloid SDS-soluble CsgB that can be found in the agar below macrocolonies. CsgB was detected by SDS-PAGE and immunoblotting.
A. CsgB was visualized in samples derived from macrocolonies grown on salt-free LB for 1 or 3 days without or with 300 mg $ml^{-1}$ phloretin as indicated. Sample treatment with hexafluoroisopropanol (HFIP) was used to solubilize SDS-insoluble CsgD in the amyloid conformation.
B. CsgB was visualized in samples containing both macrocolony cell material as well as plugs from the underlying growth agar. The sample treatment was as in (A).
C. CsgB was visualized in samples containing an agar plug only that had been cleaned from the macrocolony growing on top of it. The sample treatment was as in (A). The last lane (*) shows control samples obtained from similarly treated macrocolonies of a curli-free *ΔcsgB* derivative of strain W3110. [Color figure can be viewed at wileyonlinelibrary.com]

formation by *B. subtilis* remained unaffected by those flavonoids that showed clear effects on *E. coli* and *P. aeruginosa*, but—at 28°C and concentrations of 200 μg $ml^{-1}$—naringenin and phloretin exhibited antimicrobial activity against *B. subtilis* (Fig. 7). Using lower concentrations of naringenin and phloretin (100 and 50 μg $ml^{-1}$) the growth inhibitory effect was relieved and biofilm formation by *B. subtilis* was not affected (data not shown).

Taken together, specific flavonoids were found to show species-specific effects on macrocolony biofilm formation or bacterial growth. For the Gram-negative *E. coli* and *P. aeruginosa* flavonoid-elicited effects on biofilm formation seem more pronounced at 28°C (i.e. ambient temperature), which relates to the temperature regulation of curli fibres and pEtN-cellulose (Bokranz *et al*., 2005) or of phenazine-associated effects on macrocolony morphology (Kempes *et al*., 2014) respectively. By contrast, no effects on biofilm formation of the Gram-positive soil bacterium *B. subtilis* were observed, but naringenin and phloretin exert an antimicrobial, i.e. toxic effect at 28°C.

### *Effects of flavonoids on submerged biofilms of* E. coli *and other Gram-negative and Gram-positive bacteria*

To further explore the anti-biofilm properties of these flavonoids we investigated their impact on submerged surface-associated biofilms grown in microtiter dishes. For *E. coli*, the formation of this type of biofilm, i.e. adherence to plastic surfaces, depends on flagella and type 1 fimbriae (Pratt and Kolter, 1999). Biofilm formation in the absence

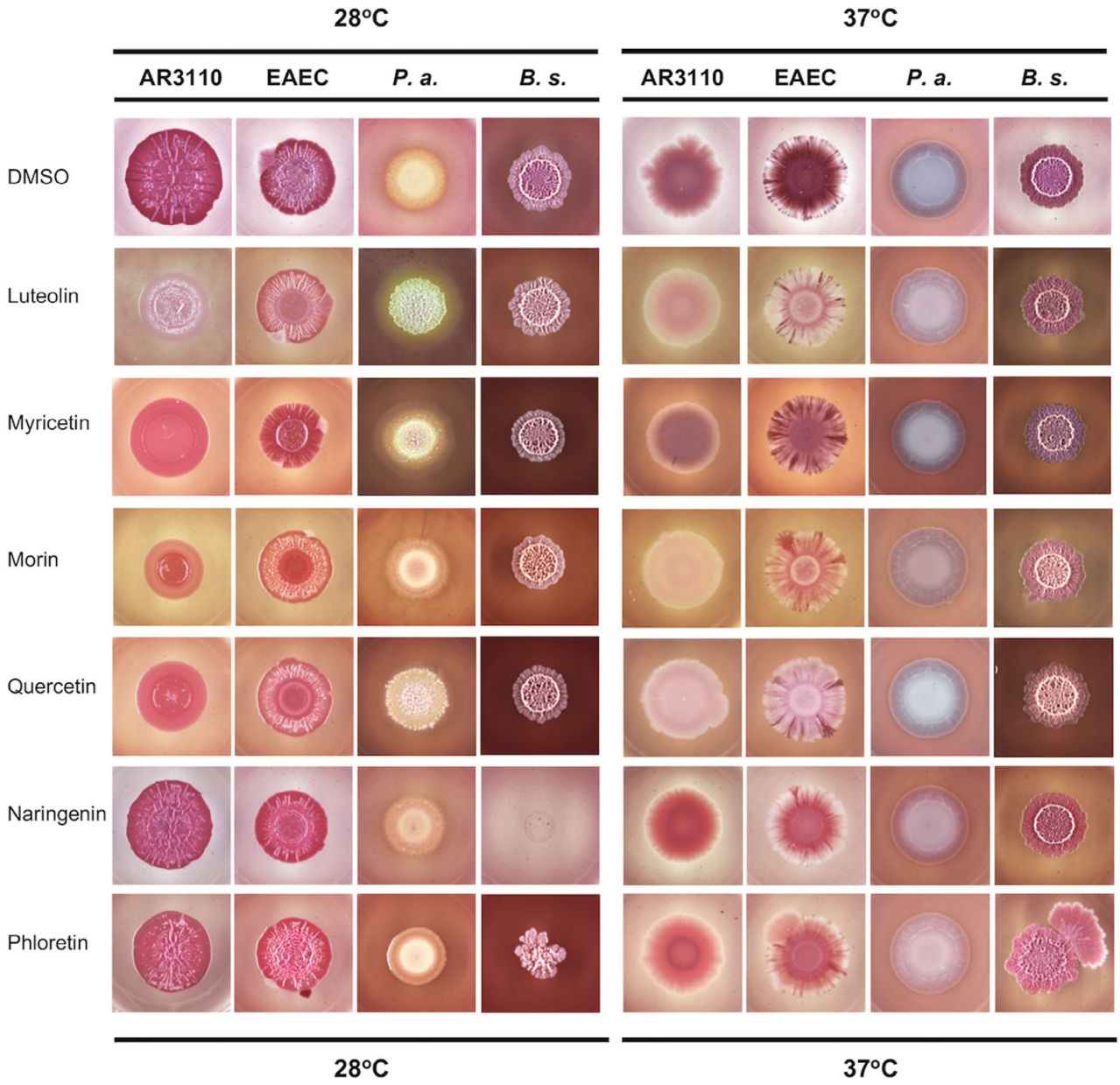


**Fig. 7.** Macrocolony biofilms of Gram-negative and Gram-positive bacteria in the presence and absence of flavonoids. Images show macrocolony biofilms of strains *E. coli* K12 strain AR3110, the enteroaggregative *E. coli* (EAEC) strain 55989, *P. aeruginosa* (*P. a.*) strain PA14 and *B. subtilis* (*B. s.*) strain NCIB 3610, grown for 5 days at 28°C or 37°C on CR plates in the absence or presence of the indicated flavonoids (200 μg $ml^{-1}$).

or presence of 200 μg $ml^{-1}$ flavonoids (at 28°C and 37°C) was quantified using crystal violet (CV) staining of bacterial biomass adhering to the walls of microtiter dishes after 24 h of growth (measuring CV absorbance at 595 nm, $Abs_{595}$; Fig. 8). To distinguish between the effects of flavonoids on biofilm formation and on bacterial growth, we also monitored the overall optical density at 578 nm during bacterial growth in the microtiter dishes ($OD_{578}$).

The addition of flavonoids to the *E. coli* K-12 strain AR3110 growing in microtiter dishes at 28°C showed weak effects only, with slightly reduced CV absorbance not indicating biofilm-specific effects as this generally correlated with equally slightly reduced overall growth (Fig. 8). During growth at 37°C, effects on CV absorbance seemed somewhat stronger, suggesting a partial biofilm-reducing activity, with morin showing the strongest effect. EAEC-55989 was found to generally adhere very poorly to microtiter plastic surface, in particular at 28°C (for absolute values, see Fig. S4). Interestingly, those flavonoids that clearly interfered with curli fibre formation

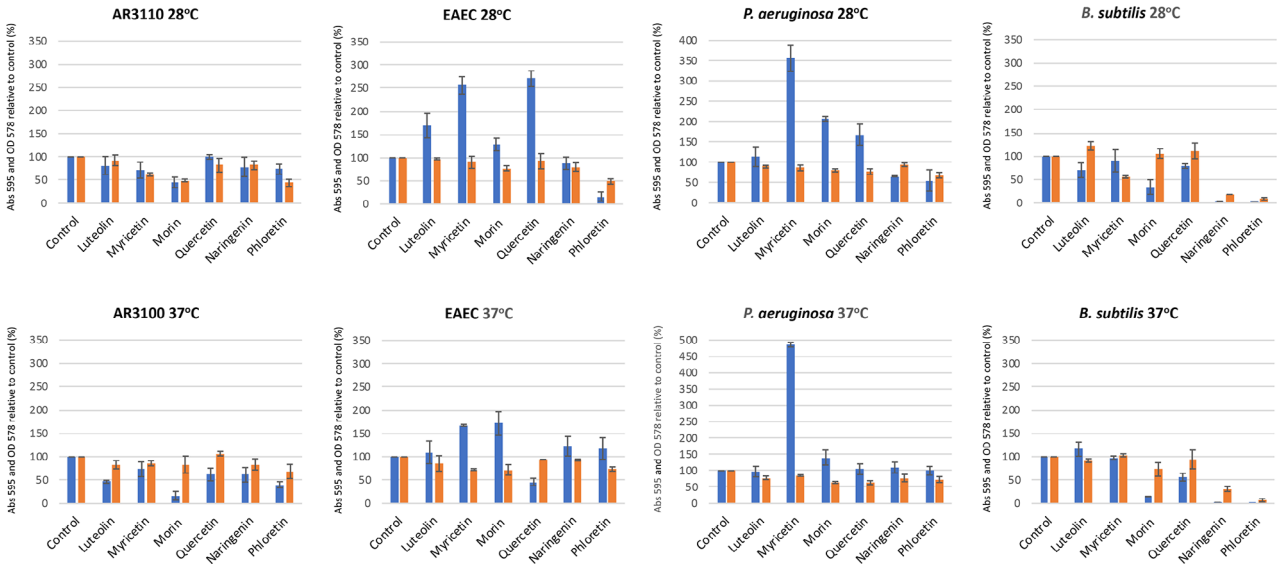


**Fig. 8.** Submerged biofilm formation by Gram-negative and Gram-positive bacteria in the absence or presence of flavonoids. Strains were the same as described in the legend to Fig. 7. Biofilm mass adhered to the microtiter dish walls was quantified by CV staining and measuring absorbance at 595 nm ($Abs_{595}$; blue bars). Bacterial growth was monitored by measuring optical density at 578 nm ($OD_{578}$; red bars). The results were derived from at least three biological replicates and are presented as the mean percentage relative to the flavonoid-free controls, with error bars as standard deviation. The absolute values for CV absorbance and $OD_{578}$ were within a similar range, except for EAEC at 28°C, as this *E. coli* strain was found to poorly form submerged biofilms (for absolute $Abs_{595}$ values, see Fig. S4).

*in vivo* (Fig. 2) and *in vitro* (Fig. 4) could in fact somewhat promote the adherence of EAEC-55989 to the microtiter plastic surface. Myricetin, morin and quercetin could also stimulate submerged biofilm formation by *P. aeruginosa* PA14, with myricetin showing the clearest effect both at 28°C and 37°C (Fig. 8). For *B. subtilis* NCIB 3610, morin seemed to reduce submerged biofilm formation in microtiter dishes, but the most pronounced effect was again the antimicrobial effect of naringenin and phloretin that had already been observed with *B. subtilis* macrocolony biofilms.

Collectively, these data again show species- and even strain-specific effects of particular flavonoids also for submerged biofilm formation by the two Gram-negative bacteria studied here. The main effect on the Gram-positive *B. subtilis* is toxicity specifically of naringenin and phloretin which is observable in biofilms as well as in planktonic liquid cultures.

## Discussion

The starting point of this study were two ecophysiological considerations: (i) plants—like all macroorganisms—have to be able to control their surface colonization by bacterial biofilms, and (ii) enteric bacteria spend part of their life cycle in the environment, where they strongly induce two biofilms matrix components, i.e. amyloid curli fibres and pEtN-cellulose, that promote adherence to plant surfaces (Fink *et al*., 2012). The consequence should be complex chemical 'negotiations' between plants and bacteria, which can be expected to involve the production of anti-biofilm agents on the plant side, i.e. agents that might also be useful in the fight against bacterial biofilms in chronic human infections. As a major class of secondary plant compounds, to which numerous beneficial effects also for human physiology have been ascribed (Havsteen, 2002; Cushnie and Lamb, 2005, 2011; Gorniak and Bartoszewski, 2019), we chose to test representatives of widespread plant flavonoids for anti-biofilm activity, using different Gram-negative and Gram-positive bacteria and two commonly used biofilm models.

### *Distinct plant flavonoids have direct and specific anti-amyloidogenic activity and thereby inhibit the formation of enteric biofilms relevant for plant surface colonization*

Several of the flavonoids investigated here, in particular, the flavones luteolin and, to a lesser degree, naringenin as well as the flavonols myricetin, morin and quercetin were found to reduce morphogenesis of macrocolonies of commensal and pathogenic *E. coli*, indicating reduced matrix formation in these biofilms (Fig. 2). *In vitro* experiments revealed these flavonoids to prevent curli fibre formation from purified CsgA subunits, with the extended lag phase of CsgA polymerization suggesting that the flavonoids directly interfere with the early nucleation and elongation stages of CsgA amyloidogenesis (Fig. 4). Our data also indicate that these flavonoids prevent amyloid fibre formation by driving the CsgA subunits into an

off-pathway that leads to SDS-insoluble dead-end oligomers (Fig. S3) that are unable to form functional curli fibres in the biofilm matrix.

Reduced curli fibre production in macrocolony biofilms was also observed in the presence of the chalcone phloretin (at 200 μg $ml^{-1}$; Fig. 2), but unlike the other flavonoids that showed similar *in vivo* activity, phloretin rather accelerated the polymerization of purified CsgA *in vitro* (Fig. 4), suggesting a different mode of activity in the more complex *in vivo* situation, where polymerization of CsgA that newly emerges at the cell surface occurs more rapidly and controlled due to templating by CsgB (Bian and Normark, 1997). We could indeed demonstrate that macrocolony growth in the presence of phloretin resulted in the release of SDS-soluble, i.e. non-amyloid CsgB into the agar phase below the colony (Fig. 6), which can explain why efficient templating of CsgA subunits into amyloid fibres is prevented. This phloretin-specific mode of action on CsgB, which thus only indirectly affects CsgA polymerization, is probably a consequence of the more open and flexible structure of phloretin as this activity is not observed with very similar, yet structurally more constrained flavone apigenin (Fig. 3).

A comparison of molecular structures of the flavonoids (Fig. 1), which interfere directly with CsgA polymerization, suggests that at least two hydroxyl groups have to be present at the B ring (at the 3′, 4′, or 5′ positions) for efficient anti-amyloidogenic activity *in vivo* and *in vitro*, with methylation of these hydroxyl groups counteracting the activity (Fig. 3). Also, glycosylated derivatives of quercetin and naringenin (rutin and naringin respectively) showed no activity (Fig. S1). Interestingly, most flavonoids occur in glycosylated forms in plants (Cushnie and Lamb, 2011; Kumar and Pandey, 2013), but bacterial metabolism (also in our intestinal microbiota, see below) generates aglycones (Eid *et al*., 2014). This suggests that enteric bacteria in their attempt to use the sugar moieties as nutrients may actually activate these 'plant-presented' compounds, which then reduce curli fibre-mediated bacterial adherence to the plant surfaces, which can be seen as a win-win situation for both sides.

The anti-amyloidogenic activity of flavonoids along with the resulting anti-biofilm activity against enteric bacteria is similar to the previously described activity of the related polyphenol epigallocatechin gallate (EGCG) that is present in high amounts in green tea (Serra *et al*., 2016; Hengge, 2019). However, a secondary activity of EGCG—namely the activation of the $\sigma^E$-mediated stress response, which downregulates the expression of CsgD and thus matrix-related gene expression (Serra *et al*., 2016)—is not exerted by the flavonoids, as none had any significant effect on the expression of genes relevant for curli or pEtN-cellulose production (Fig. S2). Notably, these effects of flavonoids and EGCG are all triggered from outside—CsgB-facilitated CsgA polymerization occurs at the bacterial cell surface (Evans and Chapman, 2014) and the signalling pathway for activating the $\sigma^E$ response is triggered by protein folding defects in the cell envelope of Gram-negative bacteria (Ades, 2008). Extracytoplasmic primary targets are just reached more easily by small hydrophilic molecules such as flavonoids—in particular in Gram-negative bacteria, where an anti-biofilm compound would have to cross two membranes in order to hit an intracellular target. Thus, amyloidogenesis and cell envelope stress responses seem more efficient anti-biofilm targets than, e.g. the intracellular enzymes that synthesize c-di-GMP or (p)ppGpp, although these represent single highly conserved enzyme families and these second messengers nearly ubiquitously promote biofilm formation (Hengge, 2019). Also previously described specific anti-biofilm effects of distinct flavonoids seem to hit extracellular processes. For instance, in *Streptococcus pneumoniae*, quercetin inhibits sortase A activity (Wang *et al*., 2018), which is required for the function of several extracytoplasmic proteins involved in bacterial aggregation and biofilm formation, including neuraminidase A or the adhesin P1 (Besingi *et al*., 2017).

Just as EGCG, some of the flavonoids (above all luteolin, but also morin and quercetin to some extent) also reduce pEtN-cellulose in the matrix of *E. coli* macrocolony biofilms (Fig. 2), i.e. the second matrix polymer, which has also been implicated in plant surface adherence (Yaron and Römling, 2014). The underlying inhibitory mechanism has yet to be elucidated and may involve direct or indirect effects on membrane-associated cellulose biosynthesis, pEtN modification in the periplasm, transfer to the cell surface or extracellular assembly into larger fibrils (Serra and Hengge, 2019a).

### *Anti-amyloidogenic activity of flavonoids does not imply general anti-biofilm activity*

The composition and architecture of biofilms are highly diverse depending on bacterial species and even strains as well as on environmental conditions. As a consequence, broad spectrum or even general anti-biofilm agents are highly unlikely to be found. This diversity is exemplified here by our data on *E. coli* and *P. aeruginosa*. Certain flavonoids efficiently reduce amyloid curli fibres and pEtN-cellulose in macrocolony biofilms and probably also when enterics attempt to adhere to plant surfaces via these EPS components. In submerged biofilms, however, curli fibres and pEtN-cellulose are present (Besharova *et al*., 2016) but not essential for the adherence to abiotic surfaces. Rather, flagella and type 1 fimbriae are required to establish this type of biofilm that is commonly assayed in microtiter dishes (Pratt and Kolter, 1999). Consistent with these differences, flavonoids that interfere with curli fibres and

pEtN-cellulose do not reduce submerged biofilm formation by our *E. coli* K-12 strain AR3110 (Fig. 8). Strikingly, the EAEC-55989 strain, which produces particularly high amounts of curli fibres and pEtN-cellulose (Richter *et al*., 2014), showed only weak submerged biofilm formation at 28°C (Fig. S4), which significantly improved not only at 37°C (where less curli and pEtN-cellulose are made) but also at 28°C when the curli/pEtN-cellulose-inhibitory flavonoids were added (Fig. 8). This suggests that the temperature-dependent or flavonoid-mediated reduction in these matrix polymers resulted in a better exposure of flagella and/or biofilm-relevant fimbriae and therefore improved attachment to submerged surfaces. Similarly, naringenin was reported to interfere with submerged biofilm formation by EHEC O157:H7, which in this strain seems controlled by AI-2-mediated quorum sensing (Vikram *et al*., 2010), whereas naringenin had no significant effect on submerged biofilm formation by *E. coli* K-12 or EAEC (Fig. 8).

Complex effects were also observed for *P. aeruginosa* PA14, where certain flavonoids seemed to actually promote biofilm formation. Luteolin, quercetin and, to a lesser extent, also myricetin stimulated the wrinkling of macrocolony biofilms (Fig. 7), which is indicative of increased extracellular matrix production. This hyper-wrinkled phenotype was previously observed for mutants lacking phenazines, which are small diffusible redox-active molecules that balance the intracellular redox state and modulate colony biofilm morphology by inhibiting matrix production via the stimulation of c-di-GMP degradation under oxidizing conditions (Okegbe *et al*., 2014; Okegbe *et al*., 2017). In principle, these flavonoids may reduce the production or—possibly via their anti-oxidative activity—interfere with the electron-shuttling activity of the phenazines. Interestingly, luteolin even seemed to activate the production of phenazines—as visually evidenced by the green colour of the macrocolonies (Fig. 7)—which could be an attempt to compensate for compromised phenazine activity. Thus, the anti-oxidative activity of luteolin may block redox shuttling by the phenazines within macrocolony biofilms, to which cells react by synthesizing more phenazines. For submerged biofilms of *P. aeruginosa*, we observed a stimulatory effect mainly of myricetin (Fig. 8). The mechanistic basis of this biofilm-promoting activity remains to be studied.

Our data also suggest that flavonoids act differently on Gram-negative and Gram-positive bacteria. Those flavonoids with the strongest effects on *E. coli* or *P. aeruginosa* did not significantly affect growth or biofilm formation of *B. subtilis* (except for morin which seemed to reduce submerged biofilm formation; Figs 7 and 8). By contrast, naringenin and phloretin were toxic, i.e. had antimicrobial activity against *B. subtilis*, both in colonies on agar plates (mainly at low temperature) and in liquid cultures (Figs 7 and 8). The antimicrobial activity of many flavonoids against Gram-positive bacteria has been reported before (Manner *et al*., 2013; Xie *et al*., 2015; Alvarez-Martínez *et al*., 2018). Some flavonoids may target Gram-positive-specific structures or processes such as sortase A in *S. pneumoniae* (Huang *et al*., 2014), but are also known to have more general effects such as membrane-disruptive activity (Tsuchiya, 2015; Alvarez-Martínez *et al*., 2018; Gorniak and Bartoszewski, 2019). Gram-negatives could be better protected against these toxic effects because flavonoids are probably too large to efficiently pass through the porins of the outer membrane.

In conclusion, some common plant flavonoids strongly and directly interfere with the formation of biofilm-associated amyloid fibres and cellulose fibrils, which can make them potent agents against biofilms specifically characterized by these or related matrix components. Besides enteric biofilms, this may also include cariogenic oral biofilms that are known to involve amyloid formation by *S. mutans* (Besingi *et al*., 2017; Berdon-Barran *et al*., 2020). Mechanistically, however, the anti-biofilm activity of flavonoids seems as species-specific as biofilm composition and regulation are highly diverse among bacteria.

### *Potential implications of the anti-amyloidogenic activity of plant flavonoids in the human organism*

A healthy human diet contains various, usually glycosylated flavonoids originating from the leaves, fruits or other parts of diet plants. These are transformed into the aglycone derivatives by our intestinal microbiota (Marín *et al*., 2015; Braune and Blaut, 2016), with free flavonoids potentially then interfering with the production of curli fibres by enteric bacteria. Notably, CsgD synthesis and therefore curli and pEtN-cellulose production occurs only at ambient temperature (<30°C) in some *E. coli* strains, but others produce these polymers also at body temperature (Bokranz *et al*., 2005). Among the latter are EAEC, which also use biofilm formation as a mode of adhesion to epithelial cells (Harrington *et al*., 2006; Richter *et al*., 2014). As bacterial amyloids have been shown to promote human inflammatory disorders and can even trigger autoimmunity (Tükel *et al*., 2010) (Gallo *et al*., 2015), the ability of flavonoids to suppress the formation of these pro-inflammatory bacterial amyloids may contribute to the anti-inflammatory effect of certain flavonoids.

Furthermore, flavonoid activity against bacterial amyloids seems to correlate with similar activity against human toxic amyloids. Thus, myricetin, morin and quercetin as well as the related catechin EGCG interfere highly efficiently with Aβ amyloid and/or α-synuclein fibre formation (Porat *et al*., 2006; Ehrnhoefer *et al*., 2008;

Bieschke *et al*., 2010). Also, flavonoids and catechins seem to have an impact on the pathophysiology of neurodegenerative diseases and in general on memory and cognitive performance (Spencer *et al*., 2012; Williams and Spencer, 2012; Devi and Chamoli, 2020). Some of the beneficial effects of these plant polyphenols on human health may thus be related to plants using polyphenol-based strategies against bacterial biofilms containing functional amyloids.

## Experimental procedures

### *Bacterial strains and growth conditions in liquid cultures*

The nonpathogenic *E. coli* strains used in this study are derivatives of the K-12 laboratory strain W3110 (Hayashi *et al*., 2006). AR3110 is a derivative of W3110 in which pEtN-cellulose synthesis was restored by replacing a stop codon in *bcsQ* by a sense codon (Serra *et al*., 2013a). Additional derivatives of AR3110 used in this study are strain AR282, which carries a *ΔcsgB* mutation, and strain AP303, which carries *ΔcsgBA::kan* as well as *ΔbcsA* (Serra *et al*., 2013a); strain GBK5, which carries a *ΔcsgD* mutation (Mika *et al*., 2012). The *csgB*::*lacZ* and *dgcC*::*lacZ* reporter fusions are integrated in a single copy in the chromosome at the *att*(lamda) site of strain W3110 (Weber *et al*., 2006; Serra *et al*., 2013a).

In addition, the EAEC strain 55989 of the serotype O104:H4 (Mossoro *et al*., 2002; Touchon *et al*., 2009), *Pseudomonas aeruginosa* strain UCBPP-PA14 (Madsen *et al*., 2015), and *Bacillus subtilis* strain NCIB 3610 (Branda *et al*., 2001; Nye *et al*., 2017) were used in these study.

Liquid bacterial cultures were grown in LB medium under aeration at 28°C or 37°C. Bacterial growth was monitored by measuring the optical density at 578 nm ($OD_{578}$).

### *Flavonoids*

All flavonoids used in this study were purchased from Sigma-Aldrich (Germany) and stock solutions of these compounds were prepared in 100% dimethyl sulfoxide (DMSO). Therefore, all experiments were done with the proper solvent controls containing DMSO alone.

### *Growth of bacterial macrocolony biofilms*

Growth of the macrocolony biofilms was as previously described (Serra and Hengge, 2017). Briefly, 5 μl of the overnight cultures (grown in liquid LB at 37°C, therefore free of extracellular matrix) were spotted on freshly prepared agar plates containing salt-free LB supplemented with CR and Coomassie brilliant blue (40 and 20 μg $ml^{-1}$ respectively) for the detection of CR binding, which is indicative of curli and pEtN-cellulose production (these agar plates are referred to as 'CR plates'). Where indicated, plates were additionally supplemented with different concentrations of flavonoids (in concentrations given in the figure legends, dissolved in DMSO) or DMSO as a solvent control. Macrocolony biofilms on agar plates were grown at 28°C or 37°C for 5 days.

### *Growth and analysis of submerged biofilms*

Submerged biofilm assays were performed in optically clear 96-well polystyrene plates (Rotilabo-Microtest plates, flat bottom, Carl Roth, Germany). Overnight cultures were diluted into fresh LB medium to an initial $OD_{578}$ of 0.05. Appropriate volumes of compound stock solutions in DMSO were added to the respective diluted bacterial cultures up to a final concentration of 200 μg $ml^{-1}$. Two hundred microliter aliquots of these cultures, with or without compounds, were then loaded into 96-well plates, the plates were sealed with Breathe-Easy sealing membrane (Sigma-Aldrich, Germany) to prevent evaporation and cross-contamination between wells, and incubated at 28°C or 37°C without shaking. After 24 h of static incubation, the $OD_{578}$ of samples was measured with the BioTek Synergy H1 plate reader. Subsequently, non-attached cells were removed, the wells were washed three times with 300 μl double-distilled water and biofilms were quantified as previously described, with some modifications (Merritt *et al*., 2005). Cells bound to the bottom or the walls of the plates were subsequently stained with 250 μl of 0.1% CV for 30 min at room temperature. Excess CV was removed and the wells were rinsed three times with 300 μl double-distilled water and left to air dry, before the bound dye was solubilized with 300 μl of an ethanol-acetone (80:20 v/v) mixture for 1 h at room temperature, and the absorbance was measured at 595 nm ($Abs_{595}$). If the measurements were outside the dynamic range of the plate reader, the CV solutions were diluted in ethanol-acetone (80:20 v/v) mixture in a new 96-well plate.

### *Stereomicroscopy*

Macrocolony biofilms were visualized at 10× magnification with a Stemi 2000-C stereomicroscope (Zeiss; Oberkochen, Germany). Digital images were captured with an AxioCamICC3 digital camera coupled to the stereomicroscope, operated via the Axio-Vision 4.8 software (Zeiss).

### *Purification of soluble CsgA protein*

Overexpression and non-denaturing purification of C-terminal His6-tagged CsgA from bacterial supernatant was performed as previously described with some modifications (Zhou *et al*., 2013). Briefly, the expression strain

LSR12/pMC1/pMC3 was grown with shaking at 37°C to an $OD_{600}$ of 1, IPTG (0.25 mM final concentration) was added to induce CsgA production, and the cultures were incubated for additional 45 min at 37°C. Cells were pelleted by centrifugation and the filtered supernatant was stored overnight at 4°C. The purification steps were performed at 4°C and the elutes and samples were stored on ice. The filtered supernatant was flowed over a 2.5 × 10 cm column packed with 4 ml of Ni-NTA and the column was washed with KPi buffer (50 mM potassium phosphate buffer, pH 7.2). CsgA was eluted from the column using 0.1 M imidazole in KPi buffer and 0.5 M imidazole in KPi buffer in the final elution step. Fractions were collected and analysed for the presence of protein by UV280 using a NanoDrop 2000 spectrophotometer (Peqlab Biotechnologie). The combined fractions were loaded onto PD10 desalting columns (GE Healthcare), eluted with 3.5 ml KPi buffer and filtered through 0.02 μm Whatman Anotop filters (GE Healthcare). The final concentration was measured by UV280 and samples were immediately used for *in vitro* polymerization assays. The identity of CsgA was confirmed by western blot using anti-6× His tag (Biomol) and anti-CsgA antibodies (obtained from Lynette Cegelski, Stanford University).

### In vitro *CsgA polymerization*

Compound stock solutions were diluted to appropriate concentrations in KPi buffer (50 mM potassium phosphate buffer, pH 7.2). In non-treated, flat-bottom, non-binding, opaque 96-well microtiter plates (Greiner), freshly purified soluble CsgA was mixed with different concentrations of flavonoids and diluted to a final concentration of 12.5 μM in KPi buffer. Control experiments were performed with DMSO added alone and with KPi buffer containing flavonoids only. ThT was added to a final concentration of 20 μM in final sample volumes of 100 μl per well and microtiter plates were covered with adhesive sealing film (EXCEL Scientific). ThT fluorescence was measured at 495 nm (excitation 438 nm) for 16 h at 23°C, with readings every 10 min, on the BioTek Synergy H1 plate reader, to monitor amyloid formation. The plate was shaken linearly for 5 s to mix samples prior to each reading. All ThT assays were performed in triplicates with at least three biological replicates. Representative ThT kinetic graphs taken from series of at least three ThT assays each are shown.

### *Transmission electron microscopy*

Subsamples (20 μl) from the CsgA polymerization assays (see above) were applied to Formvar-coated nickel grids (Science Services GmbH, Germany), allowed to absorb for 3 min, and briefly washed with MilliQ water. Subsequently, the samples were negatively stained with 2% aqueous uranyl acetate for 90 s, staining fluid was removed with a piece of filter paper, and samples were air-dried. A Zeiss EM900 Transmission Electron Microscope operated at 80 kV and equipped with a CCD camera was used to visualize curli fibres polymerized *in vitro*.

### *SDS polyacrylamide gel electrophoresis and immunoblotting to detect CsgB in macrocolony biofilms and agar plugs*

Detection of the curli subunit CsgB in macrocolonies, in macrocolonies including the underlying agar (plugs) or from the underlying agar alone was performed as described previously (Zhou *et al*., 2013), with minor modifications. For macrocolony-only analysis, colonies were scraped off the agar plates, re-suspended in PBS, normalized by optical density (578 nm) and pelleted down. The pellets were pretreated with or without 70 μl hexafluoroisopropanol (HFIP), a strong denaturant that monomerizes curli fibres. HFIP was immediately removed by vacuum centrifugation. For plug analysis, 8-mm circular sections including colony biomass and the underlying agar, or the underlying agar alone (from which the macrocolony had been carefully scraped off) were collected from plates, treated with or without 150 μl HFIP and dried immediately by vacuum centrifugation. Macrocolony-only and plug samples were resuspended in SDS-PAGE loading buffer. SDS-PAGE was carried out in 15% acrylamide resolving gels and blotted onto 0.2 mm nitrocellulose transfer membranes. To control for potentially uneven plug-derived sample application onto SDS gels, gels were stained by Coomassie Brilliant Blue and destained with 10% acetic acid solution prior to transfer onto nitrocellulose membranes. A polyclonal serum against CsgB (kindly provided by Dr. Lynette Cegelski, Stanford University, US), goat anti-rabbit IgG alkaline phosphatase conjugate (Sigma) and a chromogenic substrate (BCIP/NBT; Boehringer Mannheim, Germany) were used for detecting CsgB protein.

### *Determination of β-galactosidase activity*

β-galactosidase activity was assayed by using *o*-nitrophenyl-β-D-galactopyranoside as a substrate and is reported as μmol of *o*-nitrophenol per min per mg of cellular protein (Miller, 1972). The experiments were done at least in triplicates and average data with error bars as standard deviations are shown in the respective figures.

**Acknowledgements**

We thank Lynette Cegelski (Stanford University) for providing us with antibodies against CsgA and CsgB and the expression strain LSR12/pMC1/pMC3 for CsgA overexpression.

This work was supported by the Berliner Sparkassenstiftung Medizin (grant awarded to R.H.).

## Author Contributions

The study was conceived and experiments were designed by M.P. and R.H.; experiments were performed by M.P., J.I.H.L., and T.S.; data were interpreted and the paper was written by M.P. and R.H. and edited by all authors.

## References


Ades, S. (2008) Regulation by destruction: design of the sigmaE envelope stress response. *Curr Opin Microbiol* **11**: 535–540.

Alvarez-Martínez, F.J., Barrajón-Catalán, E., Encinar, J.A., Rodríguez-Diaz, J.C., and Micol, V. (2018) Antimicrobial capacity of plant polyphenols against Gram-positive bacteria: a comprehensive review. *Curr Med Chem* **27**: 2576–2606.

Anderson, G.G., and O'Toole, G.A. (2008) Innate and induced resistance mechanisms of bacterial biofilms. *Curr Top Microbiol Immunol* **322**: 87–107.

Andersson, E.K., Bengtsson, C., Evans, M.L., Chorell, E., Sellstedt, M., Lindgren, A.E.G., *et al*. (2013) Modulation of curli assembly and pellicle biofilm formation by chemical and protein chaperones. *Chem Biol* **20**: 1245–1254.

Barbieri, R., Coppo, E., Marchese, A., Daglia, M., Sobarzo-Sánchez, E., Nabavi, S.F., and Nabavi, S.M. (2017) Phytochemicalsw for human disease: an update on plant-derived compounds antibacterial activity. *Microbiol Res* **196**: 44–68.

Berdon-Barran, A.L., Ocampo, S., Haider, M., Morales-Aparicio, J., Ottenberg, G., Kendall, A., *et al*. (2020) Enhanced purification coupled with biophysical analyses shows cross-beta-structure as a core building block for *Streptococcus mutans* functional amyloids. *Sci Rep* **10**: 5138.

Besharova, O., Suchanek, V.M., Hartmann, R., Drescher, K., and Sourjik, V. (2016) Diversification of gene expression during formation of static submerged biofilms in *Escherichia coli*. *Front Microbiol* **7**: 1568.

Besingi, R.N., Wenderska, I.B., Senadheera, D.B., Cvitkovitch, D.G., Long, J.R., Wen, Z.T., and Brady, L.J. (2017) Functional amyloids in *Streptococcus mutans*, their use as targets of biofilm inhibition and initial characterization of SMU_63c. *Microbiology* **163**: 488–501.

Bian, Z., and Normark, S. (1997) Nucleator function of CsgB for the assembly of adhesive surface organelles in *Escherichia coli*. *EMBO J* **16**: 5827–5836.

Bieschke, J., Russ, J., Friedrich, R.P., Ehrnhoefer, D.E., Wobst, H., Neugebauer, K., and Wanker, E.E. (2010) EGCG remodels mature alpha-synuclein and amyloid-beta fibrils and reduces cellular toxicity. *Proc Natl Acad Sci U S A* **107**: 7710–7715.

Bokranz, W., Wang, X., Tschape, H., and Römling, U. (2005) Expression of cellulose and curli fimbriae by *Escherichia coli* isolated from the gastrointestinal tract. *J Med Microbiol* **54**: 1171–1182.

Branda, S.S., González-Pastor, J.E., Ben-Yehuda, S., Losick, R., and Kolter, R. (2001) Fruiting body formation by *Bacillus subtilis*. *Proc Natl Acad Sci U S A* **98**: 11621–11626.

Braune, A., and Blaut, M. (2016) Bacterial species involved in the conversion of dietary flavonoids in the human gut. *Gut Microbes* **7**: 216–234.

Brombacher, E., Dorel, C., Zehnder, A.J.B., and Landini, P. (2003) The curli biosynthesis regulator CsgD co-ordinates the expression of both positive and negative determinants for biofilm formation in *Escherichia coli*. *Microbiology* **149**: 2847–2857.

Bulgarelli, D., Schlaeppi, K., Spaepen, S., Ver Loren van Thermaat, E., and Schulze-Lefert, P. (2013) Structure and functions of the bacterial microbiota of plants. *Annu. Rev. Plant Biol.* **64**: 807–838.

Cegelski, L., Pinkner, J.S., Hammer, N.D., Cusumano, C.K., Hung, C.S., Chorell, E., *et al*. (2009) Small-molecule inhibitors target *Escherichia coli* amyloid biogenesis and biofilm formation. *Nat Chem Biol* **5**: 913–919.

Coppo, E., and Marchese, A. (2014) Antibacterial activity of polyphenols. *Curr Pharm Biotechnol* **15**: 380–390.

Costerton, J.W., Stewart, P.S., and Greenberg, E.P. (1999) Bacterial biofilms: a common cause of persistent infections. *Science* **284**: 1318–1322.

Cushnie, T.P., and Lamb, A.J. (2005) Antimicrobial activity of flavonoids. *Int J Antimicrob Agents* **26**: 343–356.

Cushnie, T.P., and Lamb, A.J. (2011) Recent advances in understanding the antibacterial properties of flavonoids. *Int J Antimicrob Agents* **38**: 99–107.

Deshmukh, M., Evans, M.L., and Chapman, M.R. (2018) Amyloid by design: intrinsic regulation of microbial amyloid assembly. *J Mol Biol* **430**: 3631–3641.

Devi, S.A., and Chamoli, A. (2020) Polyphenols as an effective therapeutic intervention against cognitive decline during normal and pathological brain aging. *Adv Exp Med Biol* **1260**: 159–174.

Diehl, A., Roske, Y., Ball, L., Chowdhury, A., Hiller, M., Molière, N., *et al*. (2018) Structural changes of TasA in biofilms formation of *Bacillus subtilis*. *Proc Natl Acad Sci U S A* **115**: 3237–3242.

Dietrich, L.E., Okegbe, C., Price-Whelan, A., Sakhtah, H., Hunter, R.C., and Newman, D.K. (2013) Bacterial community morphogenesis is intimately linked to the intracellular redox state. *J Bacteriol* **195**: 1371–1380.

Ehrnhoefer, D.E., Bieschke, J., Boeddrich, A., Herbst, M., Masino, L., Lurz, R., *et al*. (2008) EGCG redirects amyloidogenic polypeptides into unstructured, off-pathway oligomers. *Nat Struct Mol Biol* **15**: 558–566.

Eid, N., Sumia, E., Walton, G., Corona, G., Costabile, A., Gibson, G., *et al*. (2014) The impact of date palm fruits and their component polyphenols, on gut microbial ecology, bacterial metabolites and colon cancer cell proliferation. *J Nutr Sci* **3**: e46.

Erskine, E., MacPhee, C.E., and Stanley-Wall, N.R. (2018) Functional amyloid and other protein fibers in the biofilm matrix. *J Mol Biol* **430**: 3642–3656.

Evans, M.L., and Chapman, M. (2014) Curli biogenesis: order out of disorder. *Biochim Biophys Acta* **1843**: 1551–1558.

Falcone Ferreyra, M.L., Rius, S.P., and Casati, P. (2012) Flavonoids: biosynthesis, biological functions, and biotechnological applications. *Front Plant Sci* **3**: 222.

Fink, R.C., Black, E.P., Hou, Z., Sugawara, M., Sadowsky, M.J., and Diez-Gonzalez, F. (2012) Transcriptional responses of *Escherichia coli* K-12 and O157:H7 associated with lettuce leaves. *Appl Environ Microbiol* **78**: 1752–1764.

Flemming, H.-C., and Wingender, J. (2010) The biofilm matrix. *Nat Rev Microbiol* **8**: 623–633.

Flemming, H.-C., and Wuertz, S. (2019) Bacteria and archaea on Earth and their abundance in biofilms. *Nat Rev Microbiol* **17**: 247–260.

Francolini, I., and Piozzi, F. (2019) Role of antioxidant molecules and polymers in prevention of bacterial growth and biofilm formation. *Curr Med Chem* **27**: 4882–4904.

Gallo, P.M., Rapsinski, G.J., Wilson, R.P., Oppong, G.O., Sriram, U., Goulian, M., *et al*. (2015) Amyloid-DNA composites of bacterial biofilms stimulate autoimmunity. *Immunity* **42**: 1171–1184.

García, B., Latasa, C., Solano, C., García-del Portillo, F., Gamazo, C., and Lasa, I. (2004) Role of the GGDEF protein family in *Salmonella* cellulose biosynthesis and biofilm formation. *Mol Microbiol* **54**: 264–277.

Gibson, D.L., White, A.P., Rajotte, C.M., and Kay, W.W. (2007) AgfC and AgfE facilitate extracellular thin aggregative fimbriae synthesis in *Salmonella enteritidis*. *Microbiology* **153**: 1131–1140.

Gorniak, I., and Bartoszewski, R.J.K. (2019) Comprehensive review of antimicrobial activities of plant flavonoids. *Phytochem Rev* **18**: 241–272.

Hall, C.W., and Mah, T.F. (2017) Molecular mechanisms of biofilm-based antibiotic resistance and tolerance in pathogenic bacteria. *FEMS Microbiol Rev* **41**: 276–301.

Hammer, N.D., Schmidt, J.C., and Chapman, M.R. (2007) The nucleator protein, CsgB, contains an amyloidogenic domain that directs CsgA polymerization. *Proc Natl Acad Sci U S A* **104**: 12494–12499.

Harrington, S., Dudley, E., and Nataro, J.P. (2006) Pathogenesis of enteroaggregative *Escherichia coli* infection. *FEMS Microbiol Lett* **254**: 12–18.

Havsteen, B.H. (2002) The biochemistry and medical significance of the flavonoids. *Pharmacol Ther* **96**: 67–202.

Hayashi, K., Morooka, N., Yamamoto, Y., Fujita, K., Isono, K., Choi, S., *et al*. (2006) Highly accurate genome sequences of *Escherichia coli* K-12 strains MG1655 and W3110. *Mol Syst Biol* **2**: 0007.

Hengge, R. (2009) Principles of cyclic-di-GMP signaling. *Nat Rev Microbiol* **7**: 263–273.

Hengge, R. (2011) The general stress response in Gram-negative bacteria. In *Bacterial Stress Responses*, Storz, G., and Hengge, R. (eds). Washington, DC: ASM Press, pp. 251–289.

Hengge, R. (2019) Targeting bacterial biofilms by the green tea polyphenol EGCG. *Molecules* **24**: E2403.

Hengge, R. (2020) Linking bacterial growth, survival and multicellularity - small signaling molecules as triggers and drivers. *Curr Opin Microbiol* **55**: 57–66.

Huang, P., Hu, P., Zhou, S.Y., Li, Q., and Chen, W.M. (2014) Morin inhibits sortase A and subsequence biofilm formation in *Streptococcus mutans*. *Curr Microbiol* **68**: 47–52.

Jeter, C., and Matthysse, A.G. (2005) Characterization of the binding of diarrheagenic strains of *E. coli* to plant surfaces and the role of curli in the interaction of the bacteria with alfalfa sprouts. *Mol Plant Microbe Interact* **18**: 1235–1242.

Kempes, C.P., Okegbe, C., Mears-Clarke, Z., Follows, M.J., and Dietrich, L.E. (2014) Morphological optimization for access to dual oxidants in biofilms. *Proc Natl Acad Sci U S A* **111**: 208–213.

Khameneh, B., Iranshahy, M., Soheili, V., and Bazzaz, B.S. F. (2019) Review on plant antimicrobials: a mechanistic viewpoint. *Antimicrob Res Inf Contr* **8**: 118.

Khan, M.S., and Lee, J. (2015) Novel strategies for combating pathogenic biofilms using plant products and microbial antibiotics. *Curr Pharm Biotechnol* **17**: 126–140.

Klauck, G., Serra, D.O., Possling, A., and Hengge, R. (2018) Spatial organization of different sigma factor activities and c-di-GMP signalling within the three-dimensional landscape of a bacterial biofilm. *Open Biol* **8**: 180066.

Koo, H., Allan, R.N., Howlin, R.P., Stoodley, P., and Hall-Stoodley, L. (2017) Targeting microbial biofilms: current and prospective therapeutic strategies. *Nat Rev Microbiol* **15**: 740–755.

Kumar, S., and Pandey, A.K. (2013) Chemistry and biological activities of flavonoids: an overview. *Sci World J* **2013**: 1–16.

Larsen, P., Nielsen, J.L., Dueholm, M.S., Wetzel, R., Otzen, D., and Nielsen, P.H. (2007) Amyloid adhesins are abundant in natural biofilms. *Environ Microbiol* **9**: 3077–3090.

Lee, J.-H., Regmi, S.C., Kim, J.-A., Cho, M.H., Yun, H., Lee, C.-S., and Lee, J. (2011) Apple flavonoid phloretin inhibits *Escherichia coli* O157:H7 biofilm formation and ameliorates colon inflammation in rats. *Infect Immun* **79**: 4819–4827.

Lindenberg, S., Klauck, G., Pesavento, C., Klauck, E., and Hengge, R. (2013) The EAL domain phosphodiesterase YciR acts as a trigger enzyme in a c-di-GMP signaling cascade in *E. coli* biofilm control. *EMBO J* **32**: 2001–2014.

Lu, L., Hu, W., Tian, Z., Yuan, D., Yi, G., Zhou, Y., *et al*. (2019) Developing natural products as potential anti-biofilm agents. *Chin Med* **14**: 11.

Macarisin, D., Patel, J., Bauchan, G., Giron, J.A., and Sharma, V.K. (2012) Role of curli and cellulose expression in adherence of *Escherichia coli* O157:H7 to spinach leaves. *Foodborne Pathog Dis* **9**: 160–167.

Madsen, J.S., Lin, Y.C., Squyres, G.R., Price-Whelan, A., de Santiago Torio, A., Song, A., *et al*. (2015) Facultative control of matrix production optimizes competitive fitness in *Pseudomonas aeruginosa* P14 biofilm models. *Appl Environ Microbiol* **81**: 8414–8426.

Manner, S., Skogman, M., Goeres, D., Vuorela, P., and Fallarero, A. (2013) Systematic exploration of natural and synthetic flavonoids for the inhibition of *Staphylococcus aureus* biofilms. *Int J Mol Sci* **14**: 19434–19451.

Marín, L., Miguélez, E.M., Villar, C.J., and Lombó, F. (2015) Bioavailability of dietary polyphenols and gut microbiota metabolism: antimicrobial properties. *Biomed Res Int* **2015**: 905215.

Marinelli, P., Pallares, I., Navarro, S., and Ventura, S. (2016) Dissecting the contribution of *Staphylococcus aureus* a-phenol-soluble modulins to biofilm amyloid structure. *Sci Rep* **6**: 34552.

Mathesius, U. (2018) Flavonoid functions in plants and their interactions with other organisms. *Plants (Basel)* **7**: E30.

Memariani, H., Memariani, M., and Ghasemian, A. (2019) An overview on anti-biofilm properties of quercetin against bacterial pathogens. *World J Microbiol Biotechnol* **35**: 143.

Merritt, J.H., Kadouri, D.E., and O'Toole, G.A. (2005) Growing and analyzing static biofilms. In *Current Protocols in Microbiology*, Unit 1B, p. 1. Hoboken, NJ: John Wiley & Sons, Inc.

Mika, F., Busse, S., Possling, A., Berkholz, J., Tschowri, N., Sommerfeldt, N., *et al*. (2012) Targeting of *csgD* by the small regulatory RNA RprA links stationary phase, biofilm formation and cell envelope stress in *Escherichia coli*. *Mol Microbiol* **84**: 51–65.

Miller, J.H. (1972) *Experiments in Molecular Genetics*. Cold Spring Harbor, NY: Cold Spring Harbor Laboratory.

Morgan, J.L., McNamara, J.T., and Zimmer, J. (2014) Mechanism of activation of bacterial cellulose synthase by cyclic di-GMP. *Nat Struct Mol Biol* **21**: 489–496.

Mossoro, C., Glaziou, P., Yassibanda, S., Lan, N.T., Bekondi, C., Minssart, P., *et al*. (2002) Chronic diarrhea, hemorrhagic colitis, and hemolytic uremic syndrom assicated with HEp-2 adherent *Escherichia coli* in adults infected with human immunodeficiency virus in Bangui, Central African Republic. *J Clin Microbiol* **40**: 3086–3088.

Mouradov, A., and Spangenberg, G. (2014) Flavonoids: a metabolic network mediating plants adaptation to their real estate. *Front Plant Sci* **5**: 620.

Nunes Silva, L., Zimmer, K.R., Macedo, A.J., and Silva Trentin, D. (2016) Plant natural products targeting bacterial virulence factors. *Chem Rev* **116**: 9162–9236.

Nye, T.M., Schroeder, J.W., Kearns, D.B., and Simmons, L. A. (2017) Complete genome sequence of undomesticated Bacillus subtilis strain NCIB 3610. *Genome Announc* **5**: e00364-00317.

Okegbe, C., Fields, B.L., Cole, S.J., Beierschmitt, C., Morgan, C.J., Price-Whelan, A., *et al*. (2017) Electron-shuttling antibiotics structure bacterial communities by modulating cellular levels of c-di-GMP. *Proc Natl Acad Sci U S A* **114**: E5236–E5245.

Okegbe, C., Price-Whelan, A., and Dietrich, L.E. (2014) Redox-driven regulation of microbial community morphogenesis. *Curr Opin Microbiol* **18**: 39–45.

Peach, K.C., Bray, W.M., Shikuma, N.J., Gassner, N.C., Lokey, R.S., Yildiz, F.H., and Linington, R.G. (2011) An image-based 384-well high-throughput screening method for the discovery of biofilm inhibitors in *Vibrio cholerae*. *Mol Biosyst* **7**: 1176–1184.

Perov, S., Lidor, O., Salinas, N., Golan, N., Tayeb-Fligelman, E., Deshmukh, M., *et al*. (2019) Structural insights into curli CsgA cross-β fibril architecture inspire repurposing of anti-amyloid compounds as anti-biofilm agents. *PLoS Pathog* **15**: e1007978.

Pesavento, C., Becker, G., Sommerfeldt, N., Possling, A., Tschowri, N., Mehlis, A., and Hengge, R. (2008) Inverse regulatory coordination of motility and curli-mediated adhesion in *Escherichia coli*. *Genes Dev* **22**: 2434–2446.

Pfiffer, V., Sarenko, O., Possling, A., and Hengge, R. (2019) Genetic dissection of *Escherichia coli*'s master diguanylate cyclase DgcE: role of the N-terminal MASE1 domain and direct signal input from a GTPase partner system. *PLoS Genet* **15**: e1008059.

Porat, Y., Abramowitz, A., and Gazit, E. (2006) Inhibition of amyloid fibril formation by polyphenols: structural similarity and aromatic interactions as a common inhibition mechanism. *Chem Biol Drug Des* **67**: 27–37.

Pratt, L.A., and Kolter, R. (1999) Genetic analyses of bacterial biofilm formation. *Curr Opin Microbiol* **2**: 598–603.

Rabin, N., Zheng, Y., Opoku-Tememg, C., Du, Y., Bonsu, E., and Sintim, H.O. (2015) Agents that inhibit bacterial biofilm formation. *Future Med Chem* **7**: 647–671.

Rauter, J.P., Remes, S., Heinonen, M., Hopia, A., Kahkonen, M., Kujala, T., *et al*. (2018) Nomenclature of flavonoids (IUPAC Recommendations 2017). *Pure Appl Chem* **90**: 1429–1486.

Richter, A.M., Possling, A., Malysheva, N., Yousef, K.P., Herbst, S., von Kleist, M., and Hengge, R. (2020) Local c-di-GMP signaling in the control of synthesis of the *E. coli* biofilm exopolysaccharide pEtN-cellulose. *J Mol Biol* **432**: 4576–4595.

Richter, A.M., Povolotsky, T.L., Wieler, L.H., and Hengge, R. (2014) C-di-GMP signaling and biofilm-related properties of the Shiga toxin-producing German outbreak *Escherichia coli* O104:H4. *EMBO Mol Med* **6**: 1622–1637.

Romero, D., and Kolter, R. (2014) Functional amyloids in bacteria. *Int Microbiol* **17**: 65–73.

Romero, D., Sanabria-Valentin, E., Vlamakis, H., and Kolter, R. (2013) Biofilm inhibitors that target amyloid proteins. *Chem Biol* **20**: 102–110.

Römling, U., Kjelleberg, S., Normark, S., Nyman, L., Uhlin, B.E., and Åkerlund, B. (2014) Microbial biofilm formation: a need to act. *J Intern Med* **276**: 98–110.

Römling, U., Rohde, M., Olsén, A., Normark, S., and Reinköster, J. (2000) AgfD, the checkpoint of multicellular and aggregative behaviour in *Salmonella typhimurium* regulates at least two independent pathways. *Mol Microbiol* **36**: 10–23.

Rouse, S.L., Matthews, S.J., and Dueholm, M.S. (2018) Ecology and biogenesis of functional amyloids in *Pseudomonas*. *J Mol Biol* **430**: 3685–3695.

Roy, R., Tiwari, M., Donelli, G., and Tiwari, V. (2018) Strategies for combating bacterial biofilms: a focus on anti-biofilm agents and their mechanisms of action. *Virulence* **9**: 522–554.

Salinas, N., Colletier, J.P., Moshe, A., and Landau, M. (2018) Extreme amyloid polymorphism in *Staphylococcus aureus* virulent PSM-alpha peptides. *Nat Commun* **9**: 3512.

Sarenko, O., Klauck, G., Wilke, F.M., Pfiffer, V., Richter, A. M., Herbst, S., *et al*. (2017) More than enzymes that make and break c-di-GMP - the protein interaction network of GGDEF/EAL domain proteins of *Escherichia coli*. *MBio* **8**: e01639-01e617.

Serra, D.O., and Hengge, R. (2014) Stress responses go three-dimensional - the spatial order of physiological differentiation in bacterial macrocolony biofilms. *Environ Microbiol* **16**: 1455–1471.

Serra, D.O., and Hengge, R. (2017) Experimental detection and visualization of the extracellular matrix in macrocolony biofilms. In *c-di-GMP Signaling: Methods & Protocols - Methods in Molecular Biology*, Sauer, K. (ed). New York, NY: Humana Press, Springer Nature, pp. 133–145.

Serra, D.O., and Hengge, R. (2019a) Cellulose in bacterial biofilms. In *Extracellular Sugar-Based Biopolymer Matrices*, Cohen, E., and Merzendorfer, H. (eds). Cham, Switzerland: Springer International Publishing.

Serra, D.O., and Hengge, R. (2019b) A c-di-GMP-based switch controls local heterogeneity of extracellular matrix synthesis which is crucial for integrity and morphogenesis of *Escherichia coli* macrocolony biofilms. *J Mol Biol* **431**: 4775–4793.

Serra, D.O., Klauck, G., and Hengge, R. (2015) Vertical stratification of matrix production is essential for physical integrity and architecture of macrocolony biofilms of *Escherichia coli*. *Environ Microbiol* **17**: 5073–5088.

Serra, D.O., Mika, F., Richter, A.M., and Hengge, R. (2016) The green tea polyphenol EGCG inhibits *E. coli* biofilm formation by impairing amyloid curli fibre assembly and down-regulating the biofilm regulator CsgD via the σE-dependent sRNA RybB. *Mol Microbiol* **101**: 136–151.

Serra, D.O., Richter, A.M., and Hengge, R. (2013a) Cellulose as an architectural element in spatially structured *Escherichia coli* biofilms. *J Bacteriol* **195**: 5540–5554.

Serra, D.O., Richter, A.M., Klauck, G., Mika, F., and Hengge, R. (2013b) Microanatomy at cellular resolution and spatial order of physiological differentiation in a bacterial biofilm. *MBio* **4**: e00103-00113.

Spencer, J.P., Vafeiadou, K., Williams, R.J., and Vauzour, D. (2012) Neuroinflammation: modulation by flavonoids and mechanisms of action. *Mol Aspects Med* **33**: 83–97.

Stewart, P.S., and Franklin, M.J. (2008) Physiological heterogeneity in biofilms. *Nat Rev Microbiol* **6**: 199–210.

Stowe, S.D., Richards, J.J., Tucker, A.T., Thompson, R., Melander, C., and Cavanagh, J. (2011) Anti-biofilm compounds derived from marine sponges. *Mar Drugs* **9**: 2010–2035.

Taglialegna, A., Lasa, I., and Valle, J. (2016) Amyloid structures as biofilm matrix scaffolds. *J Bacteriol* **198**: 2579–2588.

Thongsomboon, W., Serra, D.O., Possling, A., Hadjineophytou, C., Hengge, R., and Cegelski, L. (2018) Phosphoethanolamine cellulose: a naturally produced chemically modified cellulose. *Science* **359**: 334–338.

Touchon, M., Hoede, C., Tenaillon, O., Barbe, V., Baeriswyl, S., Bidet, P., *et al*. (2009) Organised genome dynamics in the *Escherichia coli* species results in highly diverse adaptive paths. *PLoS Genet* **5**: e1000344.

Tsuchiya, H. (2015) Membrane interactions of phytochemicals as their molecular mechanism applicable to the discovery of drug leads from plants. *Molecules* **20**: 18923–18966.

Tükel, C., Nishimori, J.H., Wilson, R.P., Winter, M.G., Keestra, A.M., van Putten, J.P., and Bäumler, A.J. (2010) Toll-like receptors 1 and 2 cooperatively mediate immune responses to curli, a common amyloid from enterobacterial biofilms. *Cell Microbiol* **12**: 1495–1505.

Tyler, H.L., and Triplett, E.W. (2008) Plants as a habitat for beneficial and/or human pathogenic bacteria. *Annu Rev Phytopathol* **46**: 53–73.

Vikram, A., Jesudhasan, P.R., Jayaprakasha, G.K., Pillai, S. D., and Patil, B.S. (2010) Grapefruit bioactive limonoids modulate *E. coli* O157:H7 TTSS and biofilm. *Int J Food Microbiol* **140**: 109–116.

Vorholt, J.A. (2012) Microbial life in the phyllosphere. *Nat Rev Microbiol* **10**: 828–840.

Wang, J., Song, M., Pan, J., Shen, X.F., Liu, W., Zhang, X., *et al*. (2018) Quercetin inpairs *Streptococcus pneumoniae* biofilm formation by inhibiting sortase A activity. *J Cell Mol Med* **22**: 6228–6237.

Wang, X., Smith, D.R., Jones, J.W., and Chapman, M.R. (2007) *In vitro* polymerization of a functional *Escherichia coli* amyloid protein. *J Biol Chem* **282**: 3713–3719.

Weber, H., Pesavento, C., Possling, A., Tischendorf, G., and Hengge, R. (2006) Cyclic-di-GMP-mediated signaling within the $\sigma^S$ network of *Escherichia coli*. *Mol Microbiol* **62**: 1014–1034.

Williams, R.J., and Spencer, J.P. (2012) Flavonoids, cognition and dementia: actions, mechanisms, and potential therapeutic utility for Alzheimer disease. *Free Radic Biol Med* **52**: 35–45.

Xie, Y., Yang, W., Tang, F., Chen, X., and Ren, L. (2015) Antibacterial activities of flavonoids: structure-activity relationship and mechanism. *Curr Med Chem* **22**: 132–149.

Yaron, S., and Römling, U. (2014) Biofilm formation by enteric pathogens and its role in plant colonization and persistence. *Microb Biotechnol* **7**: 496–516.

Zeng, G., Vad, B.S., Dueholm, M.S., Christiansen, G., Nilsson, M., Tolker-Nielsen, T., *et al*. (2015) Functional bacterial amyloid increases *Pseudomonas* biofilm hydrophobicity and stiffness. *Front Microbiol* **6**: 1099.

Zhou, Y., Smith, D.R., Hugnagel, D.A., and Chapman, M.R. (2013) Experimental manipulation of the microbial functional amyloid called curli. *Methods Mol Biol* **966**: 53–75.

## Supporting Information

Additional Supporting Information may be found in the online version of this article at the publisher's web-site:

**Fig. S1.** A flavone lacking the 4'-OH and 3'-OH groups (chrysin), the isoflavones with a 4'-OH group only (daidzein and genistein), glycosylated forms of quercetin and naringenin (rutin and naringin respectively) and the anthocyanidin malvidin do not affect macrocolony biofilm formation. Images show macrocolony biofilms of W3110 (which produces curli only), AR232 (pEtN-cellulose only), AR3110 (curli and pEtN-cellulose) and the growth control strains AP303 or GBK3 (unable to produce curli and pEtN-cellulose) grown for 5 days at 28°C on CR plates in the absence or presence or absence of these flavonoids at the indicated concentrations.

**Fig. S2.** Flavonoids with anti-biofilm activity do not inhibit the expression of relevant genes involved in curli and pEtN-cellulose biosynthesis. The *csgBAC* curli operon and *dgcC* (encoding a diguanylate cyclase required for pEtN-cellulose biosynthesis) are both under the transcriptional control of the *E. coli* biofilm regulator CsgD and are tested here using derivatives of strain W3110 carrying the single-copy reporter fusions *csgB*::*lacZ* and *dgcC*::*lacZ*. When cultures grown in LB reached an $OD_{578}$ of 2, the indicated flavonoids were added at their minimal macrocolony biofilm-inhibitory concentrations (see Fig. 1), with the respective control samples containing the corresponding concentrations of the solvent DMSO only. The β-galactosidase activity was measured in overnight cultures at 28°C. Notably, DMSO at a concentration above 1%

has been known to somewhat enhance matrix production (Lim *et al*. 2012. Appl. Environ. Microbiol. 78: 3369–3378), which is also visible here.

**Fig. S3.** CsgA forms SDS-insoluble oligomers in the presence of flavonoids. A. Overexpression and purification of C-terminal His6-tagged CsgA by Ni-NTA affinity chromatography. SDS-PAGE gel analysis of total cell lysate of the expression strain LSR12/pMC1/pMC3 before and after IPTG induction, wash, elution (E1 to E8, eluted with 0.1 M imidazole in KPi buffer) and final elution fractions (fE1 to fE7, eluted with 0.5 M imidazole in KPi buffer) are shown. The elution fractions were pooled, desalted using PD10 desalting columns and filtered through a 0.02 μm Whatman Anotop filter. The resulting final sample used for *in vitro* CsgA polymerization is shown in (B) (CsgA 4°C). B. Samples from *in vitro* CsgA polymerization in the absence or presence of flavonoids (as described in the legend to Fig. 4; Q stands for quercetin, Mo for morin, Myr for myricetin, Nrg for naringenin, Phl for phloretin, Lut for luteolin and cmpd for compound) were taken after 16 h incubation period and centrifuged at 16,000 x g for 20 min. The supernatant fractions were transferred to fresh tubes and 30 μl aliquots were mixed with 4xSDS sample buffer (240 mM Tris pH 6.8, 400 mM DTT, 40% glycerol, 8% sodium dodecyl sulfate, 0.02% bromophenol blue) and incubated at 95°C for 10 min. Samples were loaded onto 12% SDS-PAGE gels and stained with Coomassie blue. Soluble CsgA monomers were observed in the untreated CsgA that was kept overnight at 4°C (not allowing CsgA polymerization), but no increase in the monomeric form in the presence of flavonoids was found compared to the control (no compound, in the absence of flavonoids) after the 16 h incubation period.

**Fig. S4.** Submerged biofilm formation by species and strains used in this study. *E. coli* K12 strain AR3110, the enteroaggregative *E. coli* (EAEC) strain 55,989, *P. aeruginosa* (*P. a*.) strain PA14 and *B. subtilis* (*B. s*.) were tested for their ability to form submerged biofilm in the absence of flavonoids. As described in the legend to Fig. 8, biofilm mass adhered to the microtiter dish walls was quantified by CV staining and measuring $Abs_{595}$ (blue bars), bacterial growth was monitored by measuring $OD_{578}$ (red bars). Absolute values derived from at least 3 biological replicates with error bars as standard deviation are shown.